

12-2022

Wildlife Road Mortality Patterns in South Texas and Survey Methodology Improvement

Bradley E. Beer
The University of Texas Rio Grande Valley

Follow this and additional works at: <https://scholarworks.utrgv.edu/etd>



Part of the [Animal Sciences Commons](#), and the [Biology Commons](#)

Recommended Citation

Beer, Bradley E., "Wildlife Road Mortality Patterns in South Texas and Survey Methodology Improvement" (2022). *Theses and Dissertations*. 1124.
<https://scholarworks.utrgv.edu/etd/1124>

This Thesis is brought to you for free and open access by ScholarWorks @ UTRGV. It has been accepted for inclusion in Theses and Dissertations by an authorized administrator of ScholarWorks @ UTRGV. For more information, please contact justin.white@utrgv.edu, william.flores01@utrgv.edu.

WILDLIFE ROAD MORTALITY PATTERNS IN SOUTH TEXAS AND SURVEY
METHODOLOGY IMPROVEMENT

A Thesis

by

BRADLEY E. BEER

Submitted in Partial Fulfillment of the
Requirements for the Degree of
MASTER OF SCIENCE

Major Subject: Biology

The University of Texas Rio Grande Valley

December 2022

WILDLIFE ROAD MORTALITY PATTERNS IN SOUTH TEXAS AND SURVEY
METHODOLOGY IMPROVEMENT

A Thesis
by
BRADLEY E. BEER

COMMITTEE MEMBERS

Dr. Richard J. Kline
Chair of Committee

Dr. John H. Young Jr.
Member of Committee

Dr. Karl S. Berg
Member of Committee

December 2022

Copyright 2022 Bradley E. Beer

All Rights Reserved

ABSTRACT

Beer, Bradley E., Wildlife Road Mortality Patterns in South Texas and Survey Methodology Improvement. Master of Science (MS), December, 2022, 96 pp., 9 tables, 17 figures, references, 78 titles.

Mortalities of wildlife caused by collisions with vehicles along roads are increasing in prevalence, threatening the existence of various species and populations. A better understanding of how mortalities change in response to natural and anthropogenic variables and efficient methods of obtaining mortality data are essential to mitigating such mortalities. This thesis investigates several key elements to improving road mortality surveys in south Texas. First, it was found that road mortality survey counts did not change under a pandemic-related lockdown and that 2 mortality survey observers detect more mortalities than 1. Analysis of brown pelican groundings on Texas State Highway 48 showed increased groundings with higher wind speed, lower air temperature, and lower air pressure. A pelican mortality mitigation effort was determined to have succeeded and use of an extensive citizen science dataset was validated. Lastly, road mortality video survey methodology was improved using more advanced cameras and optimized camera positions.

DEDICATION

This thesis is dedicated to my family and my soon-to-be wife. They have supported me in all respects while studying, collecting data, and writing my thesis. I am grateful to them beyond measure.

ACKNOWLEDGMENTS

I thank my advisor, Dr. Richard J. Kline, for his immense support throughout graduate school and especially with the planning and writing of this thesis. I thank the other two members of my graduate committee, Dr. Karl Berg and Dr. John Young Jr. for their assistance refining my thesis and reviewing my defense. I am grateful for the work of all members of the Kline lab past and present for their contributions to my own work. Much of the data in this thesis were collected by other lab members. I give special thanks to research associate Kevin Ryer for guidance and support and past student Trinity Livingston for her vast contributions serving as the basis for part of my thesis. I thank Stephanie Bilodeau of the Coastal Bend Bays & Estuaries Program for organizing brown pelican rescue volunteer work and for generously sharing data related to that work. I thank John Maresh of the Texas Department of Transportation and Dr. Andrew Birt of the Texas A&M Texas Transportation Institute for assisting me with designing methodology for understanding brown pelican road mortalities and for sharing data with me.

TABLE OF CONTENTS

	Page
ABSTRACT.....	iii
DEDICATION.....	iv
ACKNOWLEDGMENTS.....	v
TABLE OF CONTENTS.....	vi
LIST OF TABLES.....	viii
LIST OF FIGURES.....	ix
CHAPTER I: INTRODUCTION.....	1
CHAPTER II. WILDLIFE ROAD MORTALITIES AND COVID-19.....	4
Introduction.....	4
Methods.....	6
Results.....	13
Discussion.....	15
CHAPTER III. BROWN PELICAN ROAD MORTALITIES.....	18
Introduction.....	18
Methods.....	20
Results.....	25
Discussion.....	27

CHAPTER IV. ROAD MORTALITY VIDEO SURVEY METHODOLOGY AND	
IMPROVEMENTS	30
Introduction.....	30
Methods.....	32
Results.....	35
Discussion	36
CHAPTER V. CONCLUSION.....	40
REFERENCES	43
APPENDIX A.....	56
APPENDIX B.....	77
BIOGRAPHICAL SKETCH	96

LIST OF TABLES

	Page
Table 1: Wildlife Road Mortality Species Groups	58
Table 2: Wildlife Road Mortalities by Observation Period SIMPER.....	65
Table 3: Wildlife Road Mortalities by Number of Observers SIMPER (“All”).....	68
Table 4: Wildlife Road Mortalities by Number of Observers Mann-Whitney <i>U</i> Tests.....	70
Table 5: Wildlife Road Mortalities by Observation Period Binary Logistic Regression Model Ranking	71
Table 6: Wildlife Road Mortalities by Observation Period Top-ranked Binary Logistic Regression Model	72
Table 7: Wildlife Road Mortalities by Number of Observers Negative Binomial Regression Model Ranking	73
Table 8: Wildlife Road Mortalities by Number of Observers Top-ranked Negative Binomial Regression Model	74
Table 9: Wildlife Road Mortality Video Survey Methodology Comparisons.....	75

LIST OF FIGURES

	Page
Figure 1: Kline Lab Wildlife Road Mortality Survey Map	79
Figure 2: Wildlife Road Mortalities by Number of Observers Median Tests	80
Figure 3: Monthly Road Mortality Surveys by Number of Observers	81
Figure 4: Brown Pelican Road Mortality Survey Density Map.....	82
Figure 5: Concrete Traffic Barrier and T2P Railing.....	83
Figure 6: T2P Railing.....	84
Figure 7: Comparison of Brown Pelican Mortality Survey and Citizen Science Datasets.....	85
Figure 8: Weather Variable Plots.....	86
Figure 9: Brown Pelican Grounding Count Model Predicted Means Scatterplots	87
Figure 10: Livingston (2019) Camera Positions.....	88
Figure 11: Tested Camera Positions	89
Figure 12: Best Camera Positions Visual Comparison (Front)	90
Figure 13: Best Camera Positions Visual Comparison (Right)	91
Figure 14: Front FOV: Livingston (2019) Versus Best Tested	92
Figure 15: Right FOV: Livingston (2019) Versus Best Tested	93
Figure 16: Best Camera Positions by Speed.....	94
Figure 17: DroneViewer GPS Track.....	95

CHAPTER I

INTRODUCTION

Worldwide, roads serve important roles for transportation of humans and goods. As human populations grow, more roads are built to accommodate them. For this reason, road coverage worldwide is increasing and is predicted to increase (Meijer et al. 2018). Road development is of concern to global and regional biodiversity as roads directly degrade and destroy habitats, impede the dispersal of wildlife, and may lead to wildlife mortalities via motor vehicle traffic (Bennett 2017).

The death of individual animals has greater potential to impact a population when a population is small and the constituents are genetically similar (Hedrick and Kalinowski 2000), which is the case for ocelots (*Leopardus pardalis*) existing in Texas (Janecka and Honeycutt 2009). Ocelots are state and federally endangered and remain in the USA in only 2 populations in south Texas consisting of less than 80 individuals (Tewes 2019). Less than one quarter of these ocelots make up the population nearest Texas State Highway (SH) 100 (Figure 1), residing on Laguna Atascosa National Wildlife Refuge (LANWR). Ocelot-vehicle collisions is a leading cause of death for ocelots in south Texas, causing 45% of known mortalities 1983–2002 (Haines et al. 2005). To reduce ocelot road mortality risk in the area around LANWR and restore ocelot habitat connectivity, the Texas Department of Transportation (TxDOT) constructed 1 wildlife crossing structure (WCS) on SH 48 in 2008 (Loftus-Otway et al. 2019)

and constructed 5 WCSs on SH 100 and 8 WCS on Texas Farm to Market Road (FM) 106 in Cameron County, Texas, USA (Figure 1) between September 2016 and February 2020. WCSs allow wildlife to move from one side of a road to another without the mortal risk of crossing a road surface. The WCSs on SH 100, SH 48, and FM 106 were all underpasses of various sizes. The lab of Dr. Richard Kline at the University of Texas Rio Grande Valley (UTRGV) has performed post-WCS construction road mortality surveys on SH 100, SH 48, and FM 510 (FM 510 was monitored as a control for the roads with WCSs) beginning July 2016 and on FM 106 beginning in August 2020 (Figure 1). The methodology of these surveys will be described in Chapter II.

While mitigating ocelot mortality was the main goal of the structures, the WCSs were in potential dispersal corridors, not primary ocelot habitat (Haines et al. 2006). As of June 2021, only 1 ocelot had been captured by remote cameras near or passing through a WCS on SH 100. Additionally, as of June 2021, no ocelot had been recorded on any post-construction road mortality survey.

SH 100 is a 4-lane highway with east-west lanes that are, for the most part, separated by a concrete traffic barrier (CTB). It has a maximum speed limit of 121 kilometers/hour (km/hr). The surveyed portion of SH 100 approximately runs from the city of Los Fresnos (west) to the town of Laguna Vista (east). SH 48 is a 4-lane highway with a center CTB (for the most part) and maximum speed limit of 121 km/hr. A large lagoon, the Bahía Grande, sits adjacent to SH 48 on its north side. A channel named the Brownsville Ship Channel runs parallel to SH 48 on its south side. SH 48 connects the cities of Brownsville (west) and Port Isabel (east). FM 106 is a 2-lane east-west (overall) rural road with a maximum speed limit of 97 km/hr. The surveyed portion of FM 106 runs from census-designated place Arroyo Gardens-La Tina Ranch (west and north) to

within the first third of the surveyed portion of FM 510 (east and south). FM 510 is another 2-lane east-west rural road and has a maximum speed limit of 89 km/hr. The surveyed portion of FM 510 approximately runs from census-designated place Laureles (west) to Laguna Vista (east).

This thesis is arranged into 5 chapters. Chapter I introduced study background information and the study area. In Chapter II, the effects of the COVID-19 pandemic on wildlife road mortality surveys in south Texas will be examined. In Chapter III, the interaction of weather variables and traffic barrier types and brown pelicans being grounded by airflow over SH 48 will be examined. In Chapter IV, improvements to road mortality video survey methodology will be investigated. Chapter V serves as a conclusion for the previous chapters.

CHAPTER II

WILDLIFE ROAD MORTALITIES AND COVID-19

Introduction

The beginning of the coronavirus disease 2019 (COVID-19) pandemic in March 2020 initiated global change to existing patterns of road vehicle traffic (Khan et al. 2020, Yasin et al. 2021). Countries and localities adopted different measures to stymie the transmission of COVID-19 such as public mobility restrictions and populations voluntarily modified their travel for the same purpose (Yasin et al. 2021, Gupta et al. 2020, Kamerlin and Kasson 2020). While legal mandates and personal responses of populations varied globally, a global reduction in traffic and a global reduction human road traffic collisions occurred (though level of reduction or increase varied by country) (Yasin et al. 2021). Traffic congestion in terms of commuter delay dropped 36% between 2019 and 2020 in Brownsville, Texas (Schrank et al. 2021). Less traffic does not necessarily result in safer driving, however. Yasin et al. (2021) showed that during the COVID-19 pandemic there were higher levels of driving over speed limits during reduced traffic congestion and that drivers in the USA were more likely to drive distracted or while impaired by drugs. In Connecticut, crash rates of single vehicles increased during a stay-at-home order (despite a decrease in multivehicle crashes) (Doucette et al. 2020). Previous work in India has shown that speed limit compliance on urban arterial roads such as highways increases during peak traffic volume (Gargoum et al. 2016). This likely translates to rural roads given greater or

similar compliance in urban versus rural driving environments as respectively found through simulated driving scenarios in India (Yadav and Velaga 2021) and estimation of real traffic speed using loop detectors under the road surface in Michigan (Thornton and Lyles 1996).

Changes in traffic may have implications for wildlife road mortalities. Analyzing wildlife road mortalities during traffic reduction related to COVID-19 in 10 European countries and Israel, Bíl et al. (2020) found decreases in large mammal road mortalities in 7 countries and no statistically significant change in mortalities in the others. A reduction in wildlife road mortalities occurred in the USA states of California, Idaho, Maine, and Washington (Shilling et al. 2021). In Slovenia, there were species-specific differences in mortality rate due to COVID-19 lockdowns (Pokorny et al. 2022).

In 2020, the COVID-19 pandemic presented challenges for the road mortality surveys on SH 48, SH 100, FM 510, and FM 106 and offered unique opportunities for research in Texas and the USA. On 17 March 2020 a Cameron County judge issued a recommendation that individuals limit social gatherings, restricted travel of county government employees, ordered evaluation and then implementation of modified work schedules for county employees, and suspended deadlines for compliance with various county regulations (Cameron County Order 17 Mar 2020). Restrictions on travel and a recommendation to shelter in place was subsequently issued (Cameron County Order 20 Mar 2020), effective 22 March 2020. In turn, a series of mandatory shelter in place and movement restriction and derestriction orders (Cameron County Order 23 Mar 2020, 26 Mar 2020, 6 Apr 2020, 20 Apr 2020; Cameron County Order 24 Apr 2020*a, b*) were issued which created a lockdown in Cameron County between 23 March 2020 and 5 May 2020 followed by continued recommendation to shelter in place (Texas Exec. Order No. GA-21 2020, Cameron County Order 8 May 2020). If the lockdown shelter in place rules were properly

followed, most traffic in Cameron County would have been eliminated. The recommendations and lockdown provided an opportunity to analyze the effects of a potentially large reduction in traffic on wildlife road mortality on 4 roadways in Cameron County. To prevent COVID-19 transmission, until vaccination was available, the pandemic also required a reduction in the number of observers from 2 to 1 for road mortality surveys. While Collinson et al. (2014) found no difference in detection rate for observers in the driver seat versus the passenger seat, overall detection rate may be lowered by the observer number reduction.

The following objectives and hypotheses were addressed:

Objective 1: Wildlife Road Mortalities and COVID-19

To identify and analyze patterns in wildlife road mortalities related to the COVID-19 pandemic along the roads SH 48, SH 100, FM 510, and FM 106 in Cameron County, Texas, USA.

Hypothesis 1: COVID-19 lockdown. A lockdown for COVID-19 mandated by Cameron County, Texas, USA lowered the number of local wildlife road mortalities.

Hypothesis 2: Number of observers and size. Performing stop and exit (SE) road mortality surveys with 1 person instead of 2 lowers recorded mortality abundance.

Methods

Wildlife road mortality data from SE surveys were collected July 2016 through June 2021. During most weeks in this time range, 2 observers in a Dodge Ram 1500 pickup truck (the

passenger being seated in the front passenger seat) drove down the roads SH 48, SH 100, and FM 510. In August 2020, monitoring of FM 106 was put under the purview of the Kline lab. Beginning 17 August 2020, FM 106 was included in road mortality surveys. Herein, each individual road mortality survey encompassed all transects surveyed on a given day. All road mortality surveys were conducted weekly, with observers driving at 64 km/hr along transects (Figure 1). SH 48 and SH 100 were driven both in easterly and westerly directions each survey as mortalities could not be seen in all lanes going only one way due to the presence of CTBs. FM 106 and FM 510 were driven just one direction each survey as mortalities could be seen in both lanes while going either direction. The direction FM 106 and FM 510 were driven and the order all roads were driven were alternated weekly. The alternation lessened the chance of missing persistent mortalities with greater visibility while driving in one direction than the other. Surveys were conducted between 0800 hours and 1300 hours. The number and identity of observers and road survey order of each week's survey were recorded before beginning. While conducting surveys, the truck's hazard lights and an additional lightbar (Code3 21TR, Code3, St. Louis, MO) mounted on a BackRack (BackRack, Oakville, Canada) rack behind and above the cab were used to enhance public and observer safety. When a carcass within 10 m of the road was observed, the driver stopped the vehicle in the road shoulder and the passenger (or driver, if solo) checked ArcGIS Collector (Esri Inc., Redlands, CA, USA) on a tablet computer (2019 Samsung Galaxy Tab A, Samsung Electronics America, Inc., Ridgefield Park, NJ, USA) to see if the mortality event was new or if it had been previously recorded. Carcasses that had been recorded in a previous week had their continued presence recorded. Analyses in this study included only the first records of mortalities. a person. If new, the passenger (or driver, if solo) exited and used ArcGIS Collector to take a picture of the carcass and record information. Data recorded included

species (or most precise taxon) identification, latitude and longitude, location of carcass on the road (e.g., left or right lane), which road was being surveyed, and time and date of collection. Helmets and reflective safety vests were worn while outside the vehicle and the data collector waited for a pause in traffic to collect data if the carcass was not on or past the right shoulder. While the passenger collected data, the driver kept watch for approaching traffic, to warn the data collector of oncoming traffic if necessary. For 2-lane roads, location on the road was recorded in terms of “north” and “south” as opposed to “left” and “right.” Data collected using ArcGIS Collector were later transferred to Microsoft Excel. Several times during surveys precipitation noticeably hindered observation. In such cases, the driver pulled over until conditions became acceptable. On 4-lane roads, driving only in the right lane (unless necessary to switch to the left lane due to construction or another such issue) was crucial to obtaining consistent data. Given surveyors typically drive at a lower speed than the speed limit, slow vehicles ahead of the survey vehicle were typically not an issue. If a safety issue presented itself and passing a vehicle would mitigate the safety issue (such as a car driving slowly with hazards on), passing was performed. Otherwise, slowing down or even pulling over and waiting for a slow vehicle to move out of the area was preferred. On 2-lane roads, when driving under the speed limit, the survey vehicle was parked in the shoulder to let other vehicles pass to maintain community goodwill and for safety purposes.

Near the beginning of the COVID-19 pandemic, to impede its spread, UTRGV issued restrictions on vehicle travel with more than one person until vaccinations became available. From 23 March 2020 through 7 May 2021, 58 SE surveys were performed with 1 or 2 observers. For 46 surveys in this time period, only 1 observer performed the survey while another person

drove behind them and monitored road safety. For the other 12 surveys during this time period, 2 observers performed the survey; 1 observer was a trainee in these instances.

Statistical Analyses

COVID-19 Lockdowns. To examine differences in road mortalities due to the 2020 COVID-19 lockdown in Cameron County, Texas, USA, data across all road mortality surveys were constrained to weeks 4–27 of 2020 (20 Jan 2020 through 29 Jun 2020) to enable equal time blocks for comparison. This timeframe included surveys on SH 48, SH 100, and FM 510. Data were then divided into three observation periods encompassing the lockdown period and equal amounts of time before and after: pre-lockdown (PreL) encompassed weeks 4–11, during lockdown (DL) encompassed weeks 12–19, and post-lockdown encompassed weeks 20–27 (PostL). There were 218 mortalities recorded during weeks 4–27 of 2020. Preliminary analysis was performed in the program IBM SPSS Statistics 26 (IBM, Armonk, NY) to see if survey road should be included as a factor in analysis. The proportions of mortalities located on each individual road in each survey were compared across observation periods using a one-way analysis of variance (ANOVA). This and all analyses further in the study utilize an alpha value of 0.05 for determining statistical significance, test normality using the Shapiro-Wilk test (Shapiro and Wilk 1965), and test homogeneity of variances using Levene’s test (Levene 1960).

An ANOVA was performed on the dataset with road and observation period or just observation period as independent variables (depending on the results of the preliminary analysis) to test for differences in mean number of mortalities per survey (dependent variable) between the observation periods.

A second, modified dataset was then created to test for differences in the individual species recorded per survey between the observation periods using permutational multivariate analysis of variance (PERMANOVA) (Anderson 2001, McArdle and Anderson 2001) in the program PRIMER v7 (with the PERMANOVA+ add-on) (PRIMER-e Ltd., Ivybridge, United Kingdom). As many individual species recorded on mortality surveys were not recorded in high enough numbers to provide for robust analysis using PERMANOVA, species with relatively low numbers were consolidated into biologically relevant taxons with a goal of having groups containing at least 10 individuals recorded in the dataset (Table 1). Two unknown mortalities which could not be placed in any taxon were removed from the dataset. Coyotes (*Canis latrans*), dogs (*Canis lupus familiaris*), and unknown canids were aggregated as “canid.” Eastern cottontails (*Sylvilagus floridanus*) and black-tailed jackrabbits (*Lepus californicus*) were aggregated as “lagomorph.” Long-tailed weasels (*Neogale frenata*), striped skunks (*Mephitis mephitis*), and raccoons (*Procyon lotor*) were aggregated as “musteloid.” Birds (Aves) and snakes (Serpentes) were aggregated as “bird” and “snake” respectively. Virginia opossums (*Didelphis virginiana*) retained their own category. Groups with less than a frequency of at least 10 mortalities were excluded from further analysis: artiodactyl (Artiodactyla) ($n = 6$), felid (Felidae) ($n = 3$), nine-banded armadillo (*Dasybus novemcinctus*) ($n = 6$), rodent (Rodentia) ($n = 4$), and turtle (Testudines) ($n = 4$), resulting in 172 mortalities in the focal dataset.

Data were natural log-transformed ($\ln(x + 1)$) for each survey count to satisfy normality assumptions (Keene 1995). A resemblance matrix was generated using S_{17} (Legendre and Legendre 2012) Bray-Curtis similarity (Bray and Curtis 1957). The similarity percentages (SIMPER) (Clarke 1993) procedure was run on the matrix one-way with number of observers as a factor and using Bray-Curtis similarity as a measure.

Using the resemblance matrix, homogeneity of the dispersion was tested using permutational multivariate analysis of dispersion (PERMDISP) (Anderson 2004) using deviations from the centroid. PERMANOVA was performed with observation period as a factor, both as a main test and as pairwise tests, with unrestricted permutation of the raw data.

Number of Observers and Carcass Size. Data across all road mortality surveys were subset to 10 September 2019 through 15 June 2021. This encompassed all weeks March 2020 (when 1-observer surveys started) through the final survey in the dataset plus enough weeks prior to March 2020 to balance the number of 1 and 2 person surveys in the subset to 46 each. Data from FM 106 were not included in analysis because it was not studied during the entire range of dates. This dataset contained 835 mortalities. Species with relatively low numbers were consolidated into biologically relevant taxonomic groups with a goal of having groups containing at least 10 individuals in the dataset. Eight mortalities were unable to be categorized and were removed from the dataset. Bird wingspans ranged more than 180 centimeters (cm) between small passerines and brown pelicans. Out of concern that this large range could interfere with comparing species group observations by number of observers, a “bird” group was created but split into “large birds” and “small birds.” A wingspan measure was chosen to categorize birds as wingspan of birds tends to be longer than body length and splayed wings was observed to be common for birds struck by vehicles and exposed to wind. Average wingspan ranges for species were obtained using the Cornell Lab of Ornithology (2019) website. Using the lower number of each average wingspan range, birds ≥ 70 cm were categorized as “large” and those < 70 cm were categorized as “small.”

All non-bird species were also designated “small” or “large” so that changes in observations of mortalities of different sizes due to differing numbers of observers could be analyzed.

Published sources were used to obtain average measurements of mammals (Schmidly and Bradley 2016), turtles (Hibbitts and Hibbitts 2020), and snakes (Dixon et al. 2020).

Excepting snakes, terrestrial animals were designated “large” if they are, on average, \geq the average head-body length (42 cm, rounded down to the nearest cm) and \geq the average mass (3.15 kilograms) of a Virginia opossum in Texas, male or female. Virginia opossums were chosen as a threshold out of consideration for their abundance ($n = 107$) and potential to obscure differences in detection of the smallest animals if placed in the “small” category. Snakes have very different body shapes than other animals seen on survey. Their small girth makes them more difficult to be seen at 42 cm in head-body length. To account for this, they were designated “large” if the average of their average length range is ≥ 1 m. The 1 m threshold was chosen by doubling 42 cm and rounding to the nearest meter.

Mortalities of an unknown size ($n = 114$) were excluded from further analysis, resulting in 713 mortalities in the focal dataset. Three more datasets were created from this dataset for analysis by PERMANOVA and ANOVA: “all,” counts of each species group per survey, “total,” total mortality counts per survey, and “size,” total counts of large animals and total counts of small animals per survey. In the “all” dataset, species groups were designated “small,” “large,” or “both” based on whether the groups contain only small or large animals or both. While large turtle mortalities are possible, none were present in the dataset, so the turtle group was designated “small.”

For PERMANOVA, data were natural log-transformed ($\ln(x + 1)$) for each survey count to satisfy the assumption of normality. Resemblance matrices was generated using S_{17} Bray-Curtis

similarity for the “all” and “size” datasets and D_I (Legendre and Legendre 2012) Euclidean distance for the “total” dataset. Using the resemblance matrices, homogeneity of dispersion was tested using PERMDISP for each dataset. PERMANOVA was performed for each with number of observers as a factor, both as a main test and as pairwise tests, with unrestricted permutation of the raw data. For the “all” and “size” datasets, if significant differences were found then the SIMPER procedure was run on the transformed data one-way with number of observers as the factor using S_{17} Bray-Curtis similarity as the measure.

Differences in total, only large animal, and only small animal survey mortality counts between 1 observer and 2 observers were tested using ANOVA in SPSS. If assumptions for ANOVA failed to be met, independent-samples median tests (Mood’s median tests) (Mood 1954) and Mann-Whitney U tests (Mann and Whitney 1947) were used instead.

Results

COVID-19 Lockdown

Proportions of mortalities from each individual road did not all meet the assumption of normality (Shapiro-Wilk, FM 510, $P < 0.01$), so were normalized by applying the natural logarithmic function (Keene 1995). Using ANOVA, no difference was found in mean proportion of mortalities coming from SH 48 between observation periods ($F_{2, 20} = 1.854$, $P = 0.185$), SH 100 ($F_{2, 20} = 1.234$, $P = 0.315$), or FM 510 ($F_{2, 17} = 0.386$, $P = 0.686$). A Kruskal-Wallis H test (the data were not normal, Shapiro-Wilk, $P < 0.05$ for all observation periods for FM 510 and PreL and PostL for SH 100 and transformation could not normalize the data) was also performed on the mortality counts per survey by road (Kruskal and Wallis 1952). This showed that mortalities per survey distributions ($t_2 = 3.359$, $P = 0.186$) and medians ($t_2 = 1.779$, $P = 0.411$)

were the same across roads. Therefore, only observation period was included as an independent variable in analyses of whether a COVID-19 lockdown lowered the number of local wildlife road mortalities.

Lockdown period data were normal (Shapiro-Wilk, $P > 0.05$). The assumption of homogeneity of variances was violated (Levene's test, $P < 0.05$), so a one-way Welch's ANOVA was utilized (Welch 1951). One-way Welch's ANOVA showed that mean number of mortalities per survey were not different between the observation periods (Welch's $F_{2, 13} = 2.542$, $P = 0.116$).

The resemblance matrix data had homogeneous dispersion (PERMDISP, $F_{2, 21} = 0.85491$, $P = 0.472$) and PERMANOVA was run. No significant differences were found for each of the three combinations of observation periods; DL and PreL ($P = 0.499$); DL and PostL ($P = 0.346$); and PreL and PostL ($P = 0.099$). The SIMPER procedure (Table 2) showed that both interactions involving the observation period itself (between DL and PreL and between DL and PostL) were more similar than the PreL and PostL interaction. For that interaction, lagomorphs contributed more (23.43% versus 18.23% for DL and PreL and 18.73% for DL and PostL) and snakes contributed less to the total dissimilarity versus the other interactions (12.89% versus 20.80% for DL and PreL and 20.51% for DL and PostL).

Number of Observers and Carcass Size

Pairwise PERMDISP was run for each dataset ("all," "total," and "size") and each showed homogeneous dispersion between 1 and 2 observers for all species group counts ($F_{1,90} = 4.0155$, $P = 0.062$) and for total mortality counts ($F_{1, 90} = 0.2467$, $P = 0.621$) but not for the "size" dataset ($F_{1, 90} = 5.2896$, $P < 0.05$). PERMANOVA was therefore only performed on the "all" and

“total” datasets. There were differences in the centroids between 1 and 2 observers for both the “all” dataset ($t = 1.6735, P < 0.05$) and the “total” dataset ($t = 4.4155, P < 0.005$). SIMPER analysis of the transformed “all” dataset revealed that differences in numbers of mortalities observed with 1 observer versus 2 included substantial contribution from both large (41.41%) and small (40.76%) animal mortalities (Table 3).

Subsets of large, small, and total animal mortalities observed with 1 and 2 observers all failed tests of normality (Shapiro-Wilk, $P < 0.05$), as did various transformations of the datasets. Therefore, independent-samples median tests were used to compare median mortality counts and Mann-Whitney U tests were used to compare mortality count distributions.

A difference ($P \leq 0.001$) in the median number of mortalities recorded per survey with 1 observer versus 2 was found using an independent-samples median test (Figure 2). The same test found such difference among both only large animals ($P < 0.01$) and only small animals ($P \leq 0.001$). Mann-Whitney U tests revealed significant differences in the distribution of the 1-observer data versus 2-observer data for all animals ($U = 1617, z = 4.382, P \leq 0.001$), for just large animals ($U = 1424, z = 2.879, P < 0.01$), and for just small animals ($U = 1566, z = 4.020, P \leq 0.001$) (Table 4).

Discussion

COVID-19 Lockdown

The COVID-19 lockdown mandated by Cameron County did not lower wildlife road mortalities as compared to before or after the lockdown, so the hypothesis that it did was not supported. Mortality counts did not differ between observation periods and were closest to differing between PreL and PostL. A significant reduction in traffic perhaps didn't occur as

travel for essential activities was permitted during the lockdown and people may have ignored lockdown rules. Enforcement of lockdowns throughout the USA was lax (Ren 2020) and Cameron County was not exceptional. Roadblocks at the entrance to Port Isabel (on the eastern end of SH 48) were briefly up and alternative routes off and onto SH 48 abound. However, even if traffic did decrease, reduced traffic may have led wildlife to be less wary and attempt to cross roadways more often (Seiler and Helldin 2006). Reduced traffic may have resulted in faster driving (Yasin et al. 2020, Gargoum et al. 2016), leaving wildlife less time to avoid oncoming vehicles. Seasonal variation in animal population sizes and movement may have masked any decrease in mortalities due to the lockdown, perhaps with lagomorphs and snakes in particular (Mata et al. 2009; Canova and Balestrieri 2018). Canova and Balestrieri (2018) found eastern cottontail road mortalities in northern Italy peak during the summer. Mata et al. (2009) found rabbits in northwestern Spain utilizing wildlife crossing structures more frequently June 2002 through August 2002 versus February 2003 through March 2003 and found ophidians (including snakes and legless lacertids) only crossing during the summer months.

Number of Observers and Carcass Size

There was a significant difference in the median number of and distribution of observed mortalities between number of observers for large animals, small animals, and overall, supporting hypothesis 2. The difference in medians was stronger for small animals ($P \leq 0.001$) than for large animals ($P < 0.01$). As large animals are easier to see, they may be easier for a solo driver to spot, especially on the edge of their field of view (FOV) at any given moment. Foot surveys of birds and bats near wind turbines showed smaller species to have lower detection rates (Morrison 2002). Surveys of road mortalities in Brazil both on foot and via SE surveys

showed SE surveys involve lower detection rates than walking surveys, especially for smaller animals (Santos et al. 2016). Vehicle observers in a 3-year study of wildlife road mortalities on 5 major Tasmanian road networks failed to detect any frogs or small lizards despite their likely presence and despite over 15,000 km of total survey effort (Hobday and Minstrell (2008).

Relatively little of the difference was due to difference in mortalities of felids, the most important target taxa for road mortality research in south Texas. If such species are the main aim of a project, choosing 1 observer over 2, safety considerations notwithstanding, may be preferred. Canids and artiodactyls, other taxa that are common conservation targets, contributed relatively little to the difference as well. Seasonality may have played a role in the observed differences, so a longer study period would have been preferable. The 1-observer and 2-observer datasets differed in months covered, with the 1-observer data being biased toward earlier in the year than the 2-observer data (Figure 3).

CHAPTER III

BROWN PELICAN ROAD MORTALITIES

Introduction

Brown pelicans (*Pelecanus occidentalis*) are formerly federally (1970–2009) and state (Texas) endangered birds. Brown pelicans in Texas historically numbered approximately 5,000 individuals (U.S. Fish and Wildlife Service 2009). Breeding pairs in Texas numbered less than 10 annually 1964–1974 but grew beyond historical levels to 6,136 breeding pairs by 2009 (U.S. Fish and Wildlife Service 2009). Over the past several years, SH 48 has experienced episodic pelican mortalities adjacent to and over the Carl “Joe” Gayman Bridge (hereafter Gayman Bridge) over a channel connecting the Bahía Grande to the Brownsville Ship Channel and the bridge over San Martin Lake (hereafter “San Martin Bridge”) (Figure 4) during winter cold fronts despite no clear change in daily movement during cold fronts (Birt et al. 2021). Pelicans flying over the roadway were falling, becoming grounded and vulnerable to vehicular collisions (Birt and Gelston 2018). Pelicans cross the bridges as a part of daily movements to and from roost sites on islands in the Bahía Grande and, among other sites, the Brownsville Ship Channel (Birt et al. 2021). The local brown pelican population is estimated (based on simulated mark-resight data) to approximately range from 1,000–2,000 individuals November through March and approximately 400 mid-summer (Birt et al. 2021). Metal poles extending 12 feet above the CTBs (Figure 5) along the sides of the bridges were installed by

TxDOT in 2015 for the purpose of encouraging higher altitude bridge crossings (Birt et al. 2021), but major mortality events continued to occur. To help determine why pelicans were becoming grounded, TxDOT and the Texas A&M Transportation Institute (TTI) conducted a wind tunnel experiment, replicating the road and bridge deck. The experiment determined that the CTBs (Figure 5) along the sides of the road were affecting wind currents by causing downdrafts over the westbound lane that resulted in pelicans becoming grounded and unable to regain flight, (Birt and Gelston 2018). TxDOT and TTI then studied alternative rail types to determine which railing system would result in reduced wind turbulence while still meeting traffic safety standards. The railing type T2P (Figure 6) was found to lower the altitude of barrier-disturbed air. TxDOT elected to replace CTBs leading up to and over both sides of the Gayman and San Martin bridges with T2P railing. Construction began August 2020 and finished January 2021.

The aim of this study was to examine relationships between weather variables, the change in barrier type on both sides of SH 48, and the grounding of pelicans to further understand how to predict and mitigate pelican groundings.

The following objectives and hypotheses were addressed:

Objective 2: Brown Pelican Road Mortalities

Identify and evaluate patterns in brown pelican groundings on and along the road SH 48 in Cameron County, Texas, USA where T2P railing was installed by TxDOT in 2020 to mitigate their mortalities.

Hypothesis 1: Grounded brown pelican presence. The odds of brown pelicans being grounded on SH 48 on a given day decrease with T2P railing versus CTB and increase with increase in daily wind speed (average, minimum, maximum, and range), increase in daily gust speed (average, minimum, and maximum, and range), increase in wind direction change throughout the day, decrease in daily air pressure (average, minimum, and maximum, and range), and decrease in daily air temperature (average, minimum, and maximum, and range).

Hypothesis 2: Grounded brown pelican counts. Observed grounded brown pelican counts on SH 48 decrease with T2P railing versus CTB and increase with increase in daily wind speed (average, minimum, maximum, and range), increase in daily gust speed (average, minimum, and maximum, and range), increase in wind direction change throughout the day, decrease in daily air pressure (average, minimum, and maximum, and range), and decrease in daily air temperature (average, minimum, and maximum, and range).

Methods

Grounded Brown Pelican Presence and Counts

A subset of brown pelican mortalities from the weekly road mortality surveys on SH 48 conducted by the Kline lab were compared to data on pelican groundings collected by a group of citizen volunteers 8 December 2016 (the date of their first recording) through 28 February 2022. Citizen volunteers monitored pelican groundings and attempted to rescue living grounded pelicans during cold front events, making observation dates irregular. Observation dates occurred whenever the volunteers predicted pelican groundings would be plausible due to weather conditions. Pelican road mortality survey data collection was known to be affected by the

movement of carcasses by volunteers and TxDOT employees. Visual examination of the citizen science data showed that no major pelican mortality events indicated by the survey data appeared to have been missed by the citizen science data collection (Figure 7), so analysis proceeded solely on the finer-scale (daily) citizen science data. The amount and identity of volunteer observers varied greatly between observation dates. Observation dates differed in hours of the day spent observing pelicans but ranged from 0630 hours at earliest to 2000 hours at latest. For the purposes of this study, “daily” was hence defined as the time range 0600 hours through 2100 hours, providing a 30-minute buffer rounded up to the nearest hour. This ensured that weather data only from times potentially relevant to pelican mortalities would be used. The citizen science dataset included counts of dead pelicans (that had been grounded) and grounded pelicans that survived for each observation date. Dead and grounded counts were combined to give the total number of pelicans that were grounded on each date. Grounded pelican counts were used instead of just mortalities as volunteers present during observation periods actively interfered to save grounded pelicans. Therefore, total grounded counts from the citizen science dataset better represented the impacts of manmade structures on pelicans. The dataset held notes which revealed some discrepancies in how data was entered. The dataset was altered to alleviate these discrepancies. For example, it was noted for 31 October 2022 that 16 recorded pelicans died the previous date, so a new entry for 30 October 2022 was created and those 16 were moved from the 31 October 2022 count to the 30 October 2022 count.

Weather data were procured from the National Ocean Service station PTIT2 (26°3'40" N, 97°12'56" W) (National Oceanic and Atmospheric Administration 2022). Station PTIT2, located in Port Isabel, Texas, took readings of air temperature (C), air pressure (hectopascals (hPa)), wind speed (m/sec), gust speed (m/sec) and wind direction (degrees clockwise from true north).

Readings were reported every 6 minutes, with all but gust speed being averages over that interval. Gust speed was reported as the peak 5-8 second gust speed during the interval (National Oceanic and Atmospheric Administration 2022). This raw data over the study period (8 Dec 2016 through 28 Feb 2022) was aggregated and sets of recordings (all readings from one point in time) containing errors for any of the mentioned variables were removed. Any reading improperly recorded as the maximum possible value (e.g., 99° C for air temperature) was considered an error. Errors were present in 47,453 of 447,326 recording sets, leaving 399,873 recording sets in the dataset. There were no available data for one date, 31 October 2019, as no recordings on that date were error-free. Three grounded pelicans that were recorded on 31 October 2019 were therefore excluded from further analysis.

The corrected data were used to calculate daily averages, minima, maxima, and ranges of each type of reading except wind direction. The daily sum of the changes in wind direction between each reading was also calculated. Biological significance of results related to daily sum of changes in wind direction were interpreted more conservatively as daily differences in number of errors removed from the dataset resulted in differing daily numbers of summed recordings. All these calculated variables were visually compared to determine which ones to use in modeling (Figure 8). Gust and wind speed measures appeared to strongly correlate and past analysis of fine-scale wind data did not reveal any evidence of wind gusts that could affect pelican mortalities (Birt et al. 2021), so gust speed was not considered in analyses. Minima of air temperature, air pressure, wind speed, and gust speed appeared to closely correlate with the maxima of each respective variable, so, between those, measures relating to cold fronts (thereby being most relevant to modeling when pelicans are grounded) were chosen. These were daily maximum wind speed, daily minimum air pressure, and daily minimum air temperature. The

daily sum of the changes in wind direction between each recording, and both the daily average of and the daily range in air temperature, air pressure, and wind speed were selected to be analyzed as well.

Grounded Brown Pelican Presence

A subset of the 8 December 2016 through 28 February 2022 range was selected for modeling the interaction between weather variables and barrier type on the side of the road and whether grounded brown pelicans were observed. No grounded pelicans were recorded in the citizen science dataset 2 March through 10 October during any individual year. Adding a weeklong buffer to take into consideration possible missed groundings (the UTRGV mortality surveys found pelicans outside of the 10 October through 2 March range), the range of 9 March through 2 October (inclusive) was excluded from the dataset. In total, 847 dates were included. Grounded pelicans were recorded on 43 (approximately 5%) of these dates.

Barrier type was not analyzed with the $n = 867$ dataset. To examine the effects of barrier type, a separate dataset was created which excluded the construction period of the T2P railing (Aug 2019 through Jan 2020). This dataset included 752 survey dates. Grounded pelicans were observed on 36 of these dates. Concrete traffic barriers were present for 407 of the 752 dates and T2P railing was present for 345.

To model the different variables and grounded pelican presence and absence, a binary logistic regression was used with the larger dataset ($n = 867$). The variables included in modeling consisted of daily sum of changes in wind direction between readings, daily maximum, average, and range in wind speed, daily minimum, average, and range in air temperature, and daily minimum, average, and range in air pressure. Linearity in the logit of the variables was tested

using the Box-Tidwell procedure (Box and Tidwell 1962). Modeling began with inclusion of all variables that passed the Box-Tidwell procedure and insignificant variables were procedurally eliminated in a stepwise fashion (Yamashita et al. 2007). Colinear variables (minimum or maximum, averages, and daily ranges of the same category) were substituted for one another to find the best fit of each variable of each category for the model (Yamashita et al. 2007). The significant model with the lowest Finite Sample Corrected Akaike Information Criterion (AIC_c) value was chosen as the top-ranked model (Sugiura 1978, Hurvich and Tsai 1989). The same process was used with the $n = 752$ dataset with the inclusion of barrier type (CTB or T2P) as an additional factor.

Grounded Brown Pelican Counts

To model the different weather variables (daily maximum, average, and range in wind speed, daily minimum, average, and range in air pressure, daily minimum, average, and range in air temperature, and daily sum of the changes in wind direction between each recording) and grounded brown pelican counts, a dataset consisting only of days citizen scientists were present at the study site was used. A total of 49 dates were included. The assumptions of Poisson regression (Lovett and Flowerdew 1989) were tested. One-sample Kolmogorov-Smirnov Tests (Mijburgh and Visagie 2020) were performed to see if the variables fit the Poisson distribution. If they did not, negative binomial regression would be used to model the data (Hilbe 2012).

A separate dataset was created in which barrier type was included as a factor. This dataset excluded the construction period of the T2P railing (Aug 2019 through Jan 2020) ($n = 42$ dates). Concrete traffic barriers were present for 19 of the 42 dates and T2P railing was present for 23.

Modeling of the $n = 49$ dataset began with inclusion of all the above weather variables, excluding any that failed to meet the assumptions of the tests used. Insignificant variables were procedurally eliminated in a stepwise fashion. Colinear variables (daily minimum or maximum, daily average, and daily range of the same category) were substituted for one another to find the best fit of each variable of each category for the model. The significant model with the lowest AIC_c value was chosen as the top-ranked model. The same process was used with the $n = 42$ dataset with the inclusion of barrier type (CTB or T2P) as an additional factor.

Results

Grounded Brown Pelican Presence

The top-ranked statistically significant binary logistic regression model using the brown pelican presence dataset (including the T2P construction period, $n = 867$) had an Akaike weight value (w_i) (Wagenmakers and Farrell 2004) of 0.8609 (Table 5). The model showed decreased likelihood of grounded brown pelicans being present with increase in daily minimum air temperature (grounded presence 0.798 times as likely per 1°C increase, 95% CI [0.726, 0.870], $P < 0.001$), increase in daily average air pressure (grounded presence 0.888 times as likely per 1 hPa increase, 95% CI [0.819, 0.957], $P = 0.002$), and increased likelihood with increase in daily maximum wind speed (grounded presence 1.505 times as likely per 1 m/sec increase, 95% CI [1.355, 1.655], $P < 0.001$) (Table 6). A model using the $n = 752$ dataset was created with daily minimum air temperature, daily average air pressure, and daily maximum wind speed as covariates and barrier type as a factor. The model was significant ($P \leq 0.001$), but barrier type did not have a significant effect ($P = 0.735$). Taking this into account with a desire to avoid a gap

in the dataset, the significant model with the lowest AIC_c value using the $n = 867$ dataset was selected as the top-ranked model.

Grounded Brown Pelican Counts

Tests of whether variables fit the Poisson distribution were unable to be performed on most variables and only barrier type fit the Poisson distribution (One-Sample Kolmogorov-Smirnov, $P = 0.518$), so negative binomial regression was used. Looking at the means and variances of the variables, most variables exhibited overdispersion. Daily average and minimum air pressure exhibited underdispersion and so were not included in regression analyses (Hilbe 2012). Modeling therefore began with daily maximum, average, and range in wind speed, daily minimum, average, and range in air pressure, daily minimum, average, and range in air temperature, and daily sum of the changes in wind direction between each recording).

The top-ranked significant negative binomial regression model ($w_i = 0.3656$, $P \leq 0.001$) for grounded brown pelican counts on SH 48 (Table 7) showed association with daily minimum air temperature ($P < 0.01$), daily average air pressure ($P < 0.01$), and barrier type ($P \leq 0.001$) (Table 8). Pelican groundings decreased 80.7% (95% CI [60.0%, 90.5%]) with T2P railing versus CTB. Pelican groundings decreased 12% (95% CI [3.5%, 19.8%]) for every 1 hPa increase in daily average air pressure and 9.4% (95% CI [3.7%, 14.8%]) for every 1° C increase in daily minimum air temperature. Linear trendlines of the predicted mean pelican groundings generated by the model versus daily minimum air temperature, daily average air pressure, and barrier type were all negative (Figure 9).

Discussion

Grounded brown pelican presence on SH 48 was positively associated with increases in daily maximum wind speed and decreases in daily minimum air temperature and daily average air pressure. Other variables (daily sum of changes in wind direction, month, barrier type, daily minimum/maximum/average/range of gust speed, daily minimum/average/range in wind speed, daily maximum/average/range in air temperature, and daily minimum/maximum/range in air pressure) were not included in the final model due to collinearity or not producing a statistically significant model.

Grounded brown pelican counts on SH 48 decreased with increase in daily average air pressure, increase in daily minimum air temperature, and with T2P railing instead of CTBs. Other variables (daily sum of changes in wind direction, month, daily minimum/maximum/average/range of gust speed, daily maximum/minimum/average/range in wind speed, daily maximum/average/range in air temperature, and daily minimum/maximum/average/range in air pressure) were not included in the final model due to underdispersion, collinearity, and/or not producing a statistically significant model.

The associations align with previous analyses on pelican mortalities in the Bahía Grande which showed major mortality events to coincide with cold fronts (Birt et al. 2021). Sudden wind direction changes during cold fronts from southeast to northwest have been noted to produce “strong headwinds” for pelicans crossing to the Bahía Grande and that the proportion of a day the wind direction is between 275 and 335 degrees is associated with daily risk of pelican mortality events (Birt et al. 2021). Using directional statistics to include that proportion may help to establish a better model. Referencing known reasons for heightened risk of migratory birds

colliding with wind turbines, some possible explanations for the associations include impaired vision due to precipitation associated with lower pressure and temperature and higher wind speed, lesser ability to control flight maneuvers with stronger wind, and lower flight height in poor flying conditions (Langston and Pullan 2003).

Brown pelicans are known to intentionally soar close to waves, utilizing updrafts to reduce their energy consumption (Stokes and Lucas 2021). While gliding close to the water at their average altitude of 33 ± 5 cm (1 SD) (Hainsworth 1988), brown pelicans are approximately 15% (28 cm) to 25% (38 cm) more efficient in their use of energy due to reduced drag (Stokes and Lucas 2021). In a draft internal technical report produced for TxDOT by TTI (Birt et al. 2017), videos produced by citizen observers of pelicans crossing the Carl “Joe” Gayman Bridge in December 2016 were analyzed. The videos included examples of pelicans flying close to the CTBs (at the time) on the sides of the road. While brown pelicans are known to tend to fly at higher altitudes under windy conditions (Hainsworth 1988), striving for energy efficiency may be a factor in pelicans remaining close to the water surface prior to rising to fly over the bridges. Efficiency may also potentially be a factor in pelicans “dropping precipitously to the lagoon surface” (Birt et al. 2017) once past the bridge. Analysis of brown pelicans’ approach to and exit over the bridges (including under differing wind conditions) may give cause to explore disrupting low-altitude efficiency (on just the channel side or both sides) as a means of encouraging higher flight. Given how recently the T2P railing was installed, further collection and analysis of grounded count data should be collected before judging whether the goal of mitigating pelican mortalities with the T2P railing has been met. Pelican grounded count data may be influenced by factors not included in analysis such as variations in the size and movement of the local pelican population (Birt et al. 2021). Longer-term data would lessen bias

due to such factors. Nevertheless, replacing CTBs with T2P railing shows promise as a means of reducing (but not eliminating) pelican mortalities on SH 48.

The use of weather forecasts by pelican rescue volunteer groups to predict the potential for pelican mortalities to occur has been validated. Modeling how weather patterns by the Bahía Grande and roosting habits of brown pelicans in the Bahía Grande may change over time could better inform further action for the protection of pelicans.

CHAPTER IV

ROAD MORTALITY VIDEO SURVEY METHODS AND IMPROVEMENTS

Introduction

SE surveys are a common (Smith and van der Ree 2015) road mortality survey method that involves driving road transects at set speeds and visually recording mortality observations. The method presents challenges for safety and is time consuming when stopping and exiting the vehicle to identify road mortalities. An alternative method, video surveys decrease observer risk and reduce total labor by allowing 1 person to safely survey instead of 2. Video surveys may also raise mortality detection rate and the species richness and diversity of detected mortalities, mitigating the known bias of driving surveys against smaller animals (Langen et al. 2007, Livingston 2019). Wildlife mortality analyses often face the issue of a lack of robust data, especially for smaller species (Bíl and Andrásik 2020, Bíl et al. 2021). This is true in Texas, where TxDOT has had to rely on the TxDOT Crash Records Information System (CRIS) when investigating wildlife road mortality mitigation strategies (Loftus-Otway et al. 2019). TxDOT acknowledges that the CRIS database severely underreports wildlife-vehicle collisions. Loftus et al. (2019) discuss how the use of mobile apps by both the general public and by government employees to report wildlife-vehicle collisions shows promise regarding increasing accuracy of data available. More collision incident data would, of course, prove beneficial to analysis of wildlife road mortalities. However, the implementation of mobile app reporting systems would

not necessarily address the underreporting of smaller animals. Road mortality video surveys may be able to serve that need in the road ecology community.

Livingston (2019) performed video surveys on SH 100 and FM 510 in Cameron County, Texas, USA by attaching two GoPro Hero5 Black (GoPro, Inc., San Mateo, CA, USA) cameras to the survey vehicle and driving the same SH 100 and FM 510 transects driven for the SE surveys at 89 km/hr. The cameras were set to record video at 4k resolution (3,840 by 2,160 pixels) and 30 frames per second (FPS). Cameras with microSD cards were attached to the survey truck with suction cup mounts and a separate global positioning system (GPS) unit (Garmin GPSMAP[®] 64s, Garmin Ltd., Schaffhausen, Switzerland) was used to record tracks during surveys. One camera was placed in the upper-left portion of the survey vehicle windshield and the other camera was placed in the lower-right portion of the vehicle's hood (Figure 10). When videos exceeded the maximum file size (4 gigabytes) allowed by the formatting (FAT 32) of the microSD cards, the GoPro cameras automatically saved the video file and began recording under a new file name. After the surveys, each video file for each survey were stitched together using the application DashWare (GoPro, Inc.) and a separate program was used to overlay synchronous GPS coordinates. Two reviewers then twice-reviewed the videos from both cameras at half-speed using the media player VLC (VideoLAN, Paris, France). When mortalities were spotted, the video was paused, a screenshot was taken, and the position of the carcass on the road, latitude and longitude of the point on the GPS track closest to the carcass, and mortality species or lowest taxonomic classification determinable ("unidentified" if no taxonomic classification could be determined) were recorded. Data between the 2 reviewers were compared and double-counted mortalities were removed to produce final mortality datasets for surveys.

Livingston (2019) found that video surveys present challenges in identification of road mortalities to species. In a similar study utilizing GoPro Hero3+ Black cameras (GoPro, Inc.), Prather (2017) found similar difficulty with identification to species and determined that technological limitations would need to be overcome for video surveys to find success. Livingston (2019) also noted that technological advancement may increase the viability of video road mortality surveys. Prather (2017) specifically expressed interest in the potential of cameras able to record at 60 FPS in 4k resolution. With that in mind, the use of cameras with a greater image resolution such as the GoPro Hero9 Black (GoPro, Inc.) (which can record at 60 FPS in 4k resolution) and a different camera arrangement were predicted to be able to resolve the issue of identifying road mortalities to species. Using hardware with native GPS track recording capability (e.g., the GoPro Hero9 Black) and new software for post-survey processing of videos was noted as possible means of reducing the time required for video processing.

The following objective was addressed:

Objective 3: Road Mortality Video Survey Recommendations

Develop a best-practice protocol and explain recommendations for conducting and processing video-recorded road mortality surveys.

Methods

Comparison of Hardware and Methodology

GoPro Hero9 Black cameras were used to test video recordings of road mortality surveys on SH 100, SH 48, FM 510, and FM 106 from 12 March 2021 to 25 June 2021. Cameras were placed in aluminum skeleton frames (Forevercam, Inc., Hong Kong, China) to prevent

overheating and to protect them from fall damage and debris. Portions of the frames were removed to allow the internal GPS antennae to function. On SH 48 and SH 100 (the 4-lane roads), 10 September 2019 through 15 June 2021 (the same range used to compare mortalities by number of observers), 41.45% of mortalities observed on survey were located either on the right shoulder or in the area past the right shoulder (within 10 m of the road), 15.58% were in the right lane, and the rest were on the middle line or further left. Thus, a right-facing camera giving a close look at mortalities in the right-side hotspot survey region was seen as having great potential to enhance identification. To determine an optimal methodology for video surveys, 12 different camera positions were tested (Figure 11). Camera angles with maximal coverage were visually determined by viewing the camera FOV through the application GoPro App for Android (GoPro, Inc.) on a computer tablet (2019 Samsung Galaxy Tab A) and manually manipulating the camera. Camera angles were recorded in terms relative to the vehicle as optimal angle in terms of degrees may vary between vehicles. Tested camera positions (Figure 11) included a variety of cameras facing to the left of the vehicle, to the right of the vehicle, and toward the front of the vehicle. Livingston's (2019) positions and mounts, a suction cup-mounted camera on the outside of the driver's side of the windshield (facing forward and angled slightly down and to the left) and another on the front right side of the hood (facing forward and angled slightly down and right) were tested. The windshield camera was also tested lower on the windshield. A hood camera (placed slightly closer to the windshield and slightly further right) facing right and angled down was tested. Cameras facing the left and angled slightly down and to the right and down mounted with GoPro Jaws: Flex Clamp mounts (GoPro, Inc.) were tested. They were tested while attached on either side to the walls of the cargo bed and higher up on either side clamped to the top of the rack. Two wooden poles approximately 40 cm in height (above the cab of the

truck) were tied to either end of the rack with hose clamps. Flat mounts with very high bonding adhesive (GoPro, Inc. and 3M Company, Maplewood, Minnesota, USA) were attached to the top of the poles with the adhesive. Two zip ties were slotted through the mounts and holes drilled in the pole as a failsafe. A camera on the right pole was tested facing to the right and angled down and a camera on the left pole was tested facing forward and angled slightly down. Another flat mount was zip tied to the front of the grille and a camera facing forward was tested there. A magnet-mounted (Ridic Accessories LLC, Fountain Hills, AZ, USA) camera was tested at the point on the cab furthest forward and toward the driver's side with no apparent curvature. This camera faced forward and was angled slightly down to the left.

In addition to testing camera positions and mounts, front-facing and right-facing camera positions were tested with 16 different video recording settings (Table 9). Video recording settings tested included FOV, ("linear," "wide," or "superview"), image resolution and FPS (4k and 60 or 2.7k (2,704 by 1,524 pixels) and 120), and HyperSmooth 3.0 level ("high," "on," or "off"). HyperSmooth 3.0 is a GoPro image stabilization feature with levels of "boost," "high," "on," and "off." "High" and "on" crop 10% of the FOV. "Boost" crops even more and was not tested. A 16:9 aspect ratio was used in all tested settings variations.

Comparisons were undertaken both with actual mortalities and with dummy mortalities comprising Snellen eye charts (Free Printable Paper, Toronto, Canada) taped both to the road and to cardboard boxes. Heavy items were placed in the boxes to ensure wind would not disrupt their position. Once optimal camera positions and settings were determined, testing was performed at different speeds (64 km/hr, 72 km/hr, 80 km/hr, and 89 km/hr). With optimal methodology determined, images using that methodology were qualitatively compared to images which used the methodology of Livingston (2019). Motion blur, image resolution, viewing angle and

distortion of the size and shape of carcasses, and ability to compare different video frames were considered in this comparison. Overall, the aim was to see which produces better imagery of carcasses for the purposes of maximal detection, accuracy of identification, and review speed. Video survey tests were paused during heavy precipitation as done for SE surveys. Protocol in the SE surveys regarding passing other vehicles and letting other vehicles pass was followed to mitigate safety risks and maintain consistent data collection.

Comparison of Video-processing Software

The benefits and drawbacks of the programs VLC, DroneViewer (Earthshine Software, LLC, Huntington Beach, CA, USA), and ArcGIS Pro 2.8.0 (Esri Inc.) were qualitatively compared. This was done by describing and comparing their features, complexity of user inputs required, processing throughput, and visual display quality.

ArcGIS Pro's Full Motion Video (FMV) capabilities in the ArcGIS Pro Image Analyst extension was explored as a means of playing and processing in one application. FMV in ArcGIS Pro integrates playback and mortality data entry, allowing mortalities to be marked by clicking directly in the video. FMV also allows ground features such as points and polygons to be seen in the video player view; associated data may then be entered.

Results

Through visual comparison, the optimal camera arrangement (Figure 12, Figure 13) of the tested positions and mounts was determined to be positions (Figure 11) 7a (atop a pole facing right and toward the ground) and 4b (atop the cab facing forward). Optimal angle for the right-facing camera was determined to be an angle such that the truck bed was just out of view.

Optimal angle for the front-facing camera was determined to be where the top of the FOV is the road-sky horizon and the right side of the FOV end approximately halfway across the hood of the vehicle. Optimal front-facing camera settings were determined to be 4k resolution, 60 FPS, HyperSmooth 3.0 “on,” linear FOV (including HyperSmooth 3.0: 87° horizontally, 56° vertically). Optimal right-facing camera settings were determined to be 4k resolution, 60 FPS, HyperSmooth 3.0 “on,” and wide FOV (including HyperSmooth 3.0: 109° horizontally, 63° vertically). With double the FPS as Livingston (2019) at the same resolution, all videos with new methodology provided clearer frames and a larger number of frames to examine each carcass. The ability to examine mortalities at slightly different angles with slightly different blur in different frames is of great assistance to visual identification. Versus camera positions (Figure 11) 1a and 2a, positions 4b (Figure 14) and 7a (Figure 15) feature improved carcass viewing angles, especially with 7a. No visually significant reduction in image quality was found at 89 km/hr versus lower speeds (Figure 16), so 89 km/hr (or the speed limit where the speed limit is lower than 89 km/hr) was deemed optimal.

FMV playback quality was inferior to that of DroneViewer as it constantly stuttered. Another drawback presented itself in that processing GoPro videos requires using the FMV video multiplexer geoprocessing tool (or another such tool or program) to extract geospatial metadata into a separate file accompanying the video file to make the video FMV-compliant.

Discussion

The revised methodology exhibited greater identification potential than the Livingston (2019) methodology. Of exceptional note, the right-facing camera versus the front-facing right-side camera of Livingston (2019) provided a view more conducive to identification of the almost half

of surveyed mortalities found to the right of the vehicle. Mortalities in this view are less distorted in terms of size and shape. Their features are sharper and more easily distinguishable. If one camera is desired to be used, a magnet-mounted front-facing camera is optimal but may present difficulties when it comes to identifying mortalities on the right side of the vehicle, especially past the right shoulder. In areas that typically have significant slopes on or past the left shoulder, mounting a front-facing camera on a pole on the left side of the vehicle (as with the right) should be considered as an alternative to mounting with a magnet on the cab. This allows for mortalities on slopes on the left to be seen better. However, this may distort mortalities on the right. Processing required fewer steps due to the integrated GPS location capabilities of the GoPro Hero9 Black.

With the native location data collection capabilities of the GoPro Hero9 Black, location data did not need to be manually overlaid, reducing post-survey labor. Unlike VLC, which merely plays media, DroneViewer supplies an interactable GPS track overlaid on a satellite imagery map. Any point on the track may be clicked to access the point in time in the video when the truck was at the clicked location (Figure 17). This functionality, a bird's-eye view of the tracks linked to video time, improves or may improve survey review and data recording by making it easier to quickly move backward in time to a specific area while reviewing a video, input all desired mortality data, and select portions of videos for additional review. The first noted improvement may be desired, for example, after recording data on an observed carcass. Obtaining data such as species identity may involve carefully moving frame by frame to find the best picture angle, including past the point the carcass was first observed and the video was paused. With a focus on the observed carcass, other carcasses in frame may have been missed, so the review should resume at the point when or shortly before that carcass was observed.

Understanding how far in the survey to go back may be easier for many (if not most) people with a visual transect as opposed to a mere video progress bar. Regarding the second listed improvement, mortality data may include recording items visible via satellite imagery such as road median presence and type which would not be visible to a right-facing camera.

DroneViewer may provide an easier means of recording road median data rather than referencing the front-facing video or automatedly adding median presence and type to a GIS map based on geographic location. For the third improvement, for example, to review a trainee observer's species identifications, the ability to view a map of the mortalities they located and click right before each one may be less laborious for many (if not most) people than clicking on the video progress bar to the recorded times of observed mortalities.

Even with improvements to video processing with DroneViewer, there remains much room for improvement in terms of labor. To analyze video-recorded trawls of fish off New England, other researchers developed a custom program allowing for subjects in the video to be marked and classified and that information to be written to a separate file (DeCelles et al. 2017). A similar custom program for road mortality surveys would allow mortalities to be marked and classified and write that data to a separate file for input into GIS software. Reviewing videos and marking and classifying mortalities directly within GIS software such as ArcGIS Pro but without drawbacks identified earlier is ideal, but a custom program which generates a data file for mass input would likely prove a step beyond DroneViewer.

Regarding ArcGIS Pro, playback quality may be dependent on hardware specifications. The test computer had 16 gigabytes of random-access memory (RAM). Others may wish to try using computers with more RAM. Newer versions of ArcGIS Pro and FMV may also rectify the stuttering issue. While the necessity to create a separate metadata file for FMV complicates the

review process and adds labor, the creation of such files can be automated (Nyberg 2021). Some mortality data surveyors collect involve other features that may be geospatially referenced and visualized for data entry purposes while viewing videos. For example, for SE surveys in Cameron County, fencing type on either side of the road (or lack thereof) was noted. Fencing wouldn't necessarily be visible in video surveys, however, so being able to see a line feature demarcating a section of fencing directly in the FMV player would be beneficial. Alternatively, if such features are georeferenced, it may be possible to automate addition of data to mortality points based on proximity to those features.

With wildlife road mortalities likely to increase as human infrastructure expands, surveying road mortalities to monitor populations and the success of mortality mitigation efforts will become vital to increasing numbers of species, populations, and ecosystems. Increasing the efficiency and safety of such surveys is integral to addressing their continually greater need. Video surveys have great potential at fulfilling that need and honing their methodology is not limited to what has been presented here. Road mortality video surveys are currently in their infancy. As technology improves and cheapens, video survey labor efficiency and mortality detection rate should be expected to rise.

CHAPTER V

CONCLUSION

Analysis of wildlife road mortalities before, during, and after a county lockdown for a pandemic did not support the hypothesis that mortalities would be lower during the lockdown. The COVID-19 pandemic forced a change in road mortality survey methodology from using 2 observers to 1. Analysis of survey mortality counts with differing numbers of observers supported the hypothesis that reducing the number of observers lowers the number of mortalities detected.

Modeling brown pelican groundings on SH 48 supported in some ways and failed to support in others the hypotheses that weather variables and barrier type on the sides of the road (CTB versus the T2P railing erected as a replacement with the aim of reducing brown pelican mortalities) influence brown pelican grounding patterns. The top-ranked statistically significant model of the probability of any number of pelicans being grounded on a particular day showed higher daily maximum wind speed, lower daily minimum air temperature, and lower daily average air pressure increase the probability of pelican groundings. Railing type was shown to have no effect on the probability of pelican groundings on a given day. The top-ranked statistically significant model of the number of brown pelican groundings on days with any groundings observed by citizen scientists found the number to be lower with higher daily

minimum air temperature, higher daily average air pressure, and with T2P railing instead of CTBs. Wind gust speed was hypothesized about but found to be colinear with wind speed. The sum of daily changes in wind direction was hypothesized to affect pelican mortalities but failed to be included in either model; both models did not produce significant results with its inclusion. Daily minima, maxima, averages, and ranges of variables that were not present in the final models were not included due to collinearity or underdispersion.

GoPro Hero9 Black cameras were found to be superior to GoPro Hero5 Black cameras for road mortality video surveys both in terms of video quality (i.e., species identification potential) and labor time (by allowing for faster driving with no or minimal loss in video quality). Optimal camera placement for such surveys was found to be a front-facing camera higher up on a vehicle than previously placed (atop the cab versus on the windshield and hood) to capture mortalities to the front and left of the vehicle and a right-facing camera to capture mortalities to the right of the vehicle. Use of DroneViewer over VLC provides labor advantages in terms of ease of use and time. FMV in ArcGIS Pro may prove yet more advantageous if issues with video playback functionality and visual quality are resolved.

Video surveys may one day render moot the analysis of 1 versus 2 observers in Chapter II, however, it may be beneficial to analyze mortality detections with one video reviewer versus multiple (perhaps with concurrent walking surveys as validation). Though survey recordings are large files and may be expensive to store, stored recordings may be reviewed at any time for analyses or checking on the detection skills of a reviewer. Analyzing variation between individual reviewers versus variation between SE observers may contribute to consideration of which survey type to utilize.

Incidental video surveys may be easily incorporated into the daily work of state transportations departments such as TxDOT. This only absolutely requires mounting and unmounting cameras, starting and stopping recordings, changing and charging batteries, and changing and uploading SD cards and their data. Databases of mortality video surveys can be produced which can be processed and analyzed whenever desired.

As mortality survey efficiency increases, with the same amount of effort, more mortality survey data will be obtained. Increase in mortality survey efficiency will enable more robust datasets for analyses such as in Chapter II and Chapter III. Surveying for brown pelican mortalities on SH 48 is heavily impacted by volunteer interference for the benefit of pelicans but data from those volunteers served well as an alternate source data. However, volunteer efforts to rescue pelicans on SH 48 are performed at the pleasure and ability of the local community. If they were to cease, pelican carcasses during major mortality events may still be cleared from the road by TxDOT and others. In such a circumstance, more frequent mortality surveys specifically for brown pelicans may help capture accurate mortality data. Video surveys provide a means not only for increasing survey frequency but allow comparison of pelican positions between surveys. This may allow avoidance of recording repeat mortalities as new mortalities more easily than if, as with SE, relying on one initial mortality picture to determine if a pelican is a repeat in a different position or an unrecorded mortality.

REFERENCES

- Anderson, M. J. 2001. A new method for non-parametric multivariate analysis of variance. *Australian Ecology* 26:32–46.
- Anderson, M. J. 2004. PERMDISP: a FORTRAN computer program for permutational analysis of multivariate dispersions (for any two-factor ANOVA design) using permutation tests. University of Auckland Department of Statistics, Auckland, New Zealand.
- Bennett, V. J. 2017. Effects of road density and pattern on the conservation of species and biodiversity. *Current Landscape Ecology Reports* 2:1–11.
- Bíl, M., and R. Andrášik. 2020. The effect of wildlife carcass underreporting on KDE+ hotspots identification and importance. *Journal of Environmental Management* 275:111254.
- Bíl, M., R. Andrášik, V. Cícha, A. Arnon, M. Kruuse, J. Langbein, A. Náhlik, M. Niemi, B. Pokorný, V. J. Colino-Rabanal, et al. 2021. COVID-19 related travel restrictions prevented numerous wildlife deaths on roads: a comparative analysis of results from 11 countries. *Biological Conservation* 256:109076.

Birt, A., J. Prozzi, and J. McFalls. 2017. Brown pelican mortality on road corridors in the Bahia Grande, Texas. Draft technical report. Texas Department of Transportation, Austin, Texas, USA.

Birt, A. G., and R. Gelston. 2018. Brown pelican studies on SH 48 in south Texas. Proceedings of the Texas A&M Transportation Institute 2018 Transportation Short Course, 15 October–17 October 2018, College Station, Texas, USA.

Birt, A., L. Koczur, A. Tamayo, R. Huch, and A. Rodriguez. 2021. Daily and seasonal movements of brown pelicans in the Bahía Grande Wetland Complex. Technical Report 0-6970-R1. Texas A&M Transportation Institute, College Station, Texas, USA.

Box, G. E. P., and P. W. Tidwell. 1962. Transformation of independent variables. *Technometrics* 4:531–550.

Bray, J. R., and J. T. Curtis. 1957. An ordination of upland forest communities of southern Wisconsin. *Ecological Monographs* 27:325–349.

Cameron County Order. COVID-19 first supplemental emergency management order and recommendations. 17 March 2020.

Cameron County Order. COVID-19 second supplemental emergency management order and recommendations. 20 March 2020.

Cameron County Order. Third supplemental emergency management order with mandatory countywide shelter in place. 23 March 2020.

Cameron County Order. First amended emergency management order with mandatory countywide shelter in place. 26 March 2020.

Cameron County Order. Public notice that the first amended emergency management order with mandatory countywide shelter in place remains in effect. 6 April 2020.

Cameron County Order. Emergency management order extending mandatory countywide shelter in place with lifting of certain restrictions. 20 April 2020.

Cameron County Order. Emergency management order clarifying and updating lifting of certain restrictions. 24 April 2020.

Cameron County Order. Plan to partially re-open coastal and community parks in Cameron County. 24 April 2020.

Cameron County Order. Emergency management recommendations effective May 8, 2020. 8 May 2020.

- Canova, L., and A. Balestrieri. 2019. Long-term monitoring by roadkill counts of mammal populations living in intensively cultivated landscapes. *Biodiversity and Conservation* 28:97–113.
- Clarke, K. R. 1993. Non-parametric multivariate analyses of changes in community structure. *Australian Journal of Ecology* 18:117–143
- Clevenger, A. P., and N. Waltho. 2003. Long-term, year-round monitoring of wildlife crossing structures and the importance of temporal and spatial variability in performance studies. Pages 293–302 *in* Proceedings of the International Conference on Ecology and Transportation, 24 August 2003–29 August 2003, Lake Placid, New York, USA.
- Cornell Lab of Ornithology. 2019. All About Birds. < <https://www.allaboutbirds.org/guide/>>. Accessed 19 Apr 2022.
- Collinson, W. J., D. M. Parker, R. T. F. Bernard, B. K. Reilly, and H. T. Davies-Mostert. 2014. Wildlife road traffic accidents: a standardized protocol for counting flattened fauna. *Ecology and Evolution* 4:3060–3071.
- DeCelles, G. R., E. F. Keiley, T. M. Lowery, N. M. Calabrese, and K. D. E. Stokesbury. 2017. Development of a video trawl survey system for New England groundfish. *Transactions of the American Fisheries Society* 146:462–477.

- Dixon, J. R., J. E. Werler, M. R. J. Forstner, and R. Levoy. 2020. Revised edition. The University of Texas Press, Austin, Texas, USA.
- Doucette, M. L., A. Tucker, M. E. Auguste, A. Watkins, C. Green, F. E. Pereira, K. T. Borrup, D. Shapiro, and G. Lapidus. 2020. Initial impact of COVID-19's stay-at-home order on motor vehicle traffic and crash patterns in Connecticut: an interrupted time series analysis. *Injury Prevention* 27:3–9.
- Gargoum, S. A., K. El-Basyouny, and A. Kim. 2016. Towards setting credible speed limits: identifying factors that affect driver compliance on urban roads. *Accident Analysis and Prevention* 95:138–148.
- Gupta, S., K. I. Simon, and C. Wing. 2020. Mandated and voluntary social distancing during the COVID-19 epidemic: a review. National Bureau of Economic Research, Cambridge, Massachusetts, USA.
- Haines, A. M., M. E. Tewes, and L. L. Laack. 2005. Survival and sources of mortality in ocelots. *Journal of Wildlife Management* 69:255–263.
- Haines, A. M., M. E. Tewes, L. L. Laack, J. S. Horne, and J. H. Young. 2006. A habitat-based population viability analysis for ocelots (*Leopardus pardalis*) in the United States. *Biological Conservation* 132:424–436.

- Hainsworth, F. R. 1988. Induced drag savings from ground effect and formation flight in brown pelicans. *Journal of Experimental Biology* 135:431–444.
- Hedrick, P. W., and S. T. Kalinowski. 2000. Inbreeding depression in conservation biology. *Annual Review of Ecology and Systematics* 31:139–162.
- Hibbitts, T. D., and T. L. Hibbitts. *Texas Turtles & Crocodylians: A Field Guide*. 2016. The University of Texas Press, Austin, Texas, USA.
- Hilbe, J. M. 2012. *Negative Binomial Regression*. Second edition. Cambridge University Press, Cambridge, United Kingdom.
- Hobday, A. J., and M. L. Minstrell. 2008. Distribution and abundance of roadkill on Tasmanian highways: human management options. *Wildlife Research* 35:712–726.
- Hurvich, C. M., and Tsai, C. L. 1989. Regression and time series model selection in small samples. *Biometrika* 76:297–307.
- Janecka, J. E., and R. L. Honeycutt 2009. Conservation genetics of endangered ocelot in Texas and northern Mexico. Technical Report TX E-77-R. Texas Parks and Wildlife Department, College Station, Texas, USA.

- Kamerlin, S. C. L., and P. M. Kasson. 2020. Managing coronavirus disease 2019 spread with voluntary public health measures: Sweden as a case study for pandemic control. *Clinical Infectious Diseases* 71:3174–3181.
- Keene, O. N. 1995. The log transformation is special. *Statistics in Medicine* 14:811–819.
- Khan, I., D. Shah, and S. S. Shah. 2020. COVID-19 pandemic and its positive impacts on environment: an updated review. *International Journal of Environmental Science and Technology* 18:521–530.
- Kruskal, W. H., and W. A. Wallis. 1952. Use of ranks in one-criterion variance analysis. *Journal of the American Statistical Association* 47:583–621.
- Langen, T. A., A. Machniak, E. K. Crowe, C. Mangan, D. F. Marker, N. Liddle, and B. Roden. 2007. Methodologies for surveying herpetofauna mortality on rural highways. *Journal of Wildlife Management* 71:1361–1368.
- Langston, R. H. W., and J. D. Pullan. 2003. Windfarms and birds: an analysis of the effects of windfarms on birds, and guidance on environmental assessment criteria and site selection issues. *Proceedings of the Convention on the Conservation of European Wildlife and Natural Habitats*, 1 December–4 December 2003, Strasbourg, France.

- Legendre, L., and Legendre, P. 2012. Numerical Ecology. Third edition. Elsevier B. V., Oxford, United Kingdom.
- Levene, H. 1960. Robust tests for equality of variances. Pages 278–292 *in* I. Olkin and H. B. Mann, editors. Contribution to probability and statistics. Stanford University Press, Stanford, California, USA.
- Livingston, T. D. 2019. Wildlife road mortality survey methodologies. Thesis, University of Texas Rio Grande Valley, Brownsville, Texas, USA. Mata, C., I. Hervás, J. Herranz, J. E. Malo, and F. Suárez. 2009. Seasonal changes in wildlife use of motorway crossing structures and their implication for monitoring programmes. Transportation Research Part D: Transport and Environment 14:447–452.
- Loftus-Otway, L., N. Jiang, P. Cramer, N. Oaks, D. Wilkins, K. Kockelman, and M. R. Murphy. 2019. Incorporation of wildlife crossings into TxDOT’s projects and operations. Technical Report 0-6971-1. The University of Texas at Austin Center for Transportation Research, Austin, Texas, USA.
- Lovett, A., and Flowerdew, R. 1989. Analysis of count data using Poisson regression. Professional Geographer 41:190–198.
- Mann, H. B., and D. R. Whitney. 1947. On a test of whether one of two random variables is stochastically larger than the other. Annals of Mathematical Statistics 18:50–60.

McArdle, B. H., and Anderson, M. J. 2001. Fitting multivariate models to community data: a comment on distance-based redundancy analysis. *Ecology* 82:290–297.

Meijer, J. R., M. A. J. Huijbregts, K. C. G. J. Schotten, and A. M. Schipper. 2018. Global patterns of current and future road infrastructure. *Environmental Research Letters* 13:064006.

Mijburgh, P. A., and I. J. H. Visagie. 2020. An overview of goodness-of-fit tests for the Poisson distribution. *South African Statistical Journal* 54:207–230.

Mood, A. M. 1954. On the asymptotic efficiency of certain nonparametric two-sample tests. *Annals of Mathematical Statistics* 25:514–522.

Morrison, M. 2002. Searcher bias and scavenging rates in bird/wind energy studies. Technical Report SR-500-30876. National Renewable Energy Laboratory, Golden, Colorado, USA.

National Oceanic and Atmospheric Administration. 2022. National Data Buoy Center. Historical data for station PTIT2. <https://www.ndbc.noaa.gov/station_history.php?station=ptit2>. Accessed 7 Apr 2022.

Nyberg, E. 2021. Exprodat. Using ‘dash cam’ video data in the ArcGIS platform. <<https://www.exprodat.com/blogs/using-dash-cam-video-data-in-the-arccgis-platform/>>. Accessed 22 June 2021.

- Pokorny, B., J. Cerri, and E. Bužan. 2022. Wildlife roadkill and COVID-19: A biologically significant, but heterogeneous, reduction. *Journal of Applied Ecology* 59:1291–1301.
- Prather, J. P. 2017. Bridging the gap: attempting to increase landscape connectivity using wildlife corridors in the Lost Pines ecological area of Texas. Thesis, Texas State University, San Marcos, Texas, USA.
- Ren, X. 2020. Pandemic and lockdown: a territorial approach to COVID-19 in China, Italy, and the United States. *Eurasian Geography and Economics* 61:423–434.
- Santos, R. A. L., S. M. Santos, M. Santos-Reis, A. P. Figueirido, A. Bager, L. M. S. Aguiar, and F. Ascensão. 2016. Carcass persistence and detectability: reducing the uncertainty surrounding wildlife-vehicle collision surveys. *PLoS ONE* 11:e0165608.
- Schmidly, D. J., and R. D. Bradley. 2016. *The Mammals of Texas*. Seventh edition. The University of Texas Press, Austin, Texas, USA.
- Schrank, D., L. Albert, B. Eisele, and T. Lomax. 2021. 2021 urban mobility report. Texas A&M Transportation Institute, College Station, Texas, USA.

- Seiler, A., and J. O. Helldin. 2006. Mortality in wildlife due to transportation. Pages 165–189 *in* J. Davenport and J. L. Davenport, editors. The ecology of transportation: managing mobility for the environment. Springer Science and Business Media B.V., Dordrecht, Netherlands.
- Shapiro, S. S., and M. B. Wilk. 1965. An analysis of variance test for normality (complete samples). *Biometrika* 52:591–611.
- Shilling, F., T. Nguyen, M. Saleh, M. K. Kyaw, K. Tapia, G. Trujillo, M. Bejarano, D. Waetjen, J. Peterson, G. Kalisz., et al. 2021. A reprieve from US wildlife mortality on roads during the COVID-19 pandemic. *Biological Conservation* 256:109013.
- Smith, D. J., and R. van der Ree. 2015. Field methods to evaluate the impacts of roads on wildlife. Pages 82–95 *in* van der Ree, R. D. J. Smith, and C. Grilo, editors. *Handbook of Road Ecology*. John Wiley & Sons, Ltd., Chichester, United Kingdom.
- Sugiura, N. 1978. Further analysis of the data by Akaike's information criterion and the finite corrections. *Communications in Statistics – Theory and Methods* 7:13–26.
- Tewes, M. 2019. Conservation status of the endangered ocelot in the United States—a 35-year perspective. Texas A&M University-Kingsville 37th Annual Faculty Lecture, 8 April 2019, Kingsville, Texas, USA.

Texas Department of Transportation. 2020. Bridge railing manual. Texas Department of Transportation, Austin, Texas, USA.

Texas Exec. Order No. GA-21. 5 May 2020.

Thornton, M., and R. W. Lyles. Freeway speed zones: safety and compliance issues. 1996. Transportation Research Record 1560:65–72.

U.S. Fish and Wildlife Service. 2009. Endangered and threatened wildlife and plants; removal of the brown pelican (*Pelecanus occidentalis*) from the federal list of endangered and threatened wildlife. 74 FR 59443–59472. U.S Fish and Wildlife Service Southwest Regional Office, Albuquerque, New Mexico, USA.

Wagenmakers, E. and S. Farrell. 2004. AIC model selection using Akaike weights. *Psychonomic Bulletin and Review* 11:192–196.

Welch, B. L. 1951. On the comparison of several mean values: an alternative approach. *Biometrika* 38:330–336.

Yadav, A. K., and N. R. Velaga. 2021. Investigating the effects of driving environment and driver characteristics on drivers' compliance with speed limits. *Traffic Injury Prevention* 22:201–206.

Yamashita, T., K. Yamashita, and R. Kamimura. 2007. A stepwise AIC method for variable selection in linear regression. *Communications in Statistics–Theory and Methods* 36:2395–2403.

Yasin, Y. J., M. Grivna, and F. M. Abu-Zidan. 2021. Global impact of COVID-19 pandemic on road traffic collisions. *World Journal of Emergency Surgery* 16:51.

APPENDIX A

APPENDIX A

TABLES

Table 1. Species groups in analyses of wildlife road mortalities on Texas State Highway (SH) 48, SH 100, and Texas Farm to Market Road (FM) 510 in Cameron County, Texas, USA, 10 September 2019 through 15 June 2021.

Analysis group	Common name	Scientific name	Size	<i>n</i> (Hypothesis 1) ^a	<i>n</i> (Hypothesis 2) ^b
Artiodactyl	Javelina	<i>Pecari tajacu</i>	Large	0	2
	Nilgai	<i>Boselaphus tragocamelus</i>	Large	0	4
	White-tailed deer	<i>Odocoileus virginianus</i>	Large	0	5
Bird (large)	Black skimmer	<i>Rynchops niger</i>	Large	0	1
	Black-bellied whistling duck	<i>Dendrocygna autumnalis</i>	Large	3	7
	Black-crowned night heron	<i>Nycticorax nycticorax</i>	Large	1	2
	Brown pelican	<i>Pelecanus occidentalis</i>	Large	2	63
	Caspian tern	<i>Hydroprogne caspia</i>	Large	0	2
	Crested caracara	<i>Caracara plancus</i>	Large	0	1
	Great blue heron	<i>Ardea herodias</i>	Large	0	1
	Great egret	<i>Ardea alba</i>	Large	0	1

^aA lockdown for COVID-19 mandated by Cameron County, Texas, USA lowered the number of local wildlife road mortalities.

^b Performing stop and exit road mortality surveys with 1 person instead of 2 lowers recorded mortality abundance.

Table 1, cont. Species groups in analyses of wildlife road mortalities on SH 48, SH 100, and FM 510 in Cameron County, Texas, USA, 10 September 2019 through 15 June 2021.

Analysis group	Common name	Scientific name	Size	<i>n</i> (Hypothesis 1)	<i>n</i> (Hypothesis 2)
Bird (large)	Gull (unknown)	Laridae	Large	18	38
	Gull-billed tern	<i>Gelochelidon nilotica</i>	Large	0	1
	Laughing gull	<i>Leucophaeus atricilla</i>	Large	9	55
	Osprey	<i>Pandion haliaetus</i>	Large	0	1
	Ring-billed gull	<i>Larus delawarensis</i>	Large	0	1
	Roseate spoonbill	<i>Platalea ajaja</i>	Large	0	1
	Turkey vulture	<i>Cathartes aura</i>	Large	0	1
	Vulture (unknown)	Catharidae	Large	0	1
	Yellow-crowned night heron	<i>Nyctanassa violacea</i>	Large	0	1
Bird (small)	Barn owl	<i>Tyto alba</i>	Small	9	16
	Barn swallow	<i>Hirundo rustica</i>	Small	0	1
	Belted kingfisher	<i>Megaceryle alcyon</i>	Small	0	1

Table 1, cont. Species groups in analyses of wildlife road mortalities on SH 48, SH 100, and FM 510 in Cameron County, Texas, USA, 10 September 2019 through 15 June 2021.

Analysis group	Common name	Scientific name	Size	<i>n</i> (Hypothesis 1)	<i>n</i> (Hypothesis 2)
Bird (small)	Common pauraque	<i>Nyctidromus albicollis</i>	Small	1	2
	Common yellowthroat	<i>Geothlypis trichas</i>	Small	0	1
	Eastern meadowlark	<i>Sturnella magna</i>	Small	2	9
	Golden-fronted woodpecker	<i>Melanerpes aurifrons</i>	Small	0	1
	Great-tailed grackle	<i>Quiscalus mexicanus</i>	Small	1	25
	Killdeer	<i>Charadrius vociferus</i>	Small	0	1
	Least bittern	<i>Botaurus lentiginosus</i>	Small	0	2
	Long-billed thrasher	<i>Toxostoma longirostre</i>	Small	0	2
	Mimid (unknown)	<i>Mimidae</i>	Small	0	1
	Mourning dove	<i>Zenaida macroura</i>	Small	0	2
	Nighthawk (unknown)	<i>Chordeiles spp.</i>	Small	1	1
	Northern bobwhite	<i>Colinus virginianus</i>	Small	3	10

Table 1, cont. Species groups in analyses of wildlife road mortalities on SH 48, SH 100, and FM 510 in Cameron County, Texas, USA, 10 September 2019 through 15 June 2021.

Analysis group	Common name	Scientific name	Size	<i>n</i> (Hypothesis 1)	<i>n</i> (Hypothesis 2)
Bird (small)	Northern mockingbird	<i>Mimus polyglottos</i>	Small	3	19
	Small bird (unknown)	<i>Aves</i>	Small	4	22
	Spotted sandpiper	<i>Actitis macularius</i>	Small	0	1
	Western kingbird	<i>Tyrannus verticalis</i>	Small	0	1
	Yellow-billed cuckoo	<i>Coccyzus americanus</i>	Small	0	1
Canid	Coyote	<i>Canis latrans</i>	Large	7	22
	Domestic dog	<i>Canis lupus familiaris</i>	Large	3	12
Felid	Bobcat	<i>Largeynx rufus</i>	Large	0	3
	Domestic cat	<i>Felis catus</i>	Large	0	13
Lagomorph	Black-tailed jackrabbit	<i>Largeepus californicus</i>	Small	1	8
	Eastern cottontail	<i>Sylvilagus floridanus</i>	Small	26	65
	Rabbit (unknown)	<i>Largeeporidae</i>	Small	0	1

Table 1, cont. Species groups in analyses of wildlife road mortalities on SH 48, SH 100, and FM 510 in Cameron County, Texas, USA, 10 September 2019 through 15 June 2021.

Analysis group	Common name	Scientific name	Size	<i>n</i> (Hypothesis 1)	<i>n</i> (Hypothesis 2)
Musteloid	Long-tailed weasel	<i>Mustela frenata</i>	Small	1	2
	Northern raccoon	<i>Procyon lotor</i>	Large	10	45
	Striped skunk	<i>Mephitis californium</i>	Large	6	21
Nine-banded armadillo	Nine-banded armadillo	<i>Dasypus novemcinctus</i>	Small	0	20
Rodent	Cricetid rat (unknown)	<i>Cricetidae</i>	Small	0	1
	Mexican ground squirrel	<i>Spermophilus mexicanus</i>	Small	0	1
	Murid rat (unknown)	<i>Muridae</i>	Small	0	1
	North American Beaver	<i>Castor canadensis</i>	Large	0	1
	Rodent (unknown)	<i>Rodentia</i>	Small	0	18
Snake	Bullsnake	<i>Pituophis catenifer sayi</i>	Large	0	1
	Great Plains ratsnake	<i>Elaphe emoryi</i>	Small	1	2

Table 1, cont. Species groups in analyses of wildlife road mortalities on SH 48, SH 100, and FM 510 in Cameron County, Texas, USA, 10 September 2019 through 15 June 2021.

Analysis group	Common name	Scientific name	Size	<i>n</i> (Hypothesis 1)	<i>n</i> (Hypothesis 2)
Snake	Snake (unknown)	<i>Serpentes</i>	Unknown	5	0
	Texas indigo snake	<i>Drymarchon melanurus erebennus</i>	Large	2	3
	Western coachwhip	<i>Masticophis flagellum testaceus</i>	Large	1	1
	Western diamondback rattlesnake	<i>Crotalus atrox</i>	Large	18	29
Turtle	Red-eared slider	<i>Trachemys scripta elegans</i>	Small	0	5
	Testudinidae (unknown)	<i>Testudinidae</i>	Small	0	1
	Texas spiny softshell turtle	<i>Apalone spinifera emoryi</i>	Small	0	1
	Texas tortoise	<i>Gopherus berlandieri</i>	Small	0	15
	Turtle (unknown)	<i>Testudines</i>	Small	0	6

Table 1, cont. Species groups in analyses of wildlife road mortalities on SH 48, SH 100, and FM 510 in Cameron County, Texas, USA, 10 September 2019 through 15 June 2021.

Analysis group	Common name	Scientific name	Size	<i>n</i> (Hypothesis 1)	<i>n</i> (Hypothesis 2)
Virginia opossum	Virginia opossum	<i>Didelphis virginiana</i>	Large	34	107
Total large				114	447
Total small				53	266
Total unknown				5	0
Total (all)				172	713

Table 2. SIMPER^a (Clarke 1993) results of wildlife road mortality data collected weeks 4–27 of 2020 on Texas State Highway (SH) 48, SH 100, and Texas Farm to Market Road (FM) 510 in Cameron County, Texas, USA. The data were sectioned into 3 observation periods: pre-lockdown (PreL, weeks 4–11), during the lockdown (DL, weeks 12–19), and post-lockdown (PostL, weeks 20–27). The data were transformed by $\ln(x + 1)$. Total mortality $n = 172$.

Species Group (G)	G ₁ Average Abundance	G ₂ Average Abundance	Average Dissimilarity	Contribution % ^b
Total DL (1) and PreL (2)	4.45	4.50	41.99	100.01
Snake ($n_1 = 17, n_2 = 3$)	0.95	0.26	8.73	20.80
Bird ($n_1 = 16, n_2 = 22$)	1.24	1.37	7.87	18.75
Lagomorph ($n_1 = 11, n_2 = 15$)	0.76	0.90	7.65	18.23
VA Opossum ($n_1 = 12, n_2 = 16$)	0.79	1.00	7.37	17.56
Musteloid ($n_1 = 6, n_2 = 7$)	0.45	0.57	5.65	13.46
Canid ($n_1 = 3, n_2 = 5$)	0.26	0.40	4.71	11.21

^aSimilarity percentages.

^bDo not total to 100 due to rounding.

Table 2, cont. SIMPER^a results of wildlife road mortality data collected weeks 4–27 of 2020 on SH 48, SH 100, and FM 510 in Cameron County, Texas, USA. The data were sectioned into 3 observation periods: PreL (weeks 4–11), DL (weeks 12–19), and PostL (weeks 20–27). The data were transformed by $\ln(x + 1)$. Total mortality $n = 172$.

Species Group (G)	G ₁ Average Abundance	G ₂ Average Abundance	Average Dissimilarity	Contribution % ^b
Total DL (1) and PostL (2)	4.45	2.79	49.50	100.01
Bird ($n_1 = 16, n_2 = 19$)	1.24	1.21	10.60	21.41
Snake ($n_1 = 17, n_2 = 7$)	0.95	0.53	10.15	20.51
Lagomorph ($n_1 = 11, n_2 = 1$)	0.76	0.09	9.27	18.73
Virginia Opossum ($n_1 = 12, n_2 = 6$)	0.79	0.48	8.34	16.84
Musteloid ($n_1 = 6, n_2 = 4$)	0.45	0.31	6.66	13.45
Canid ($n_1 = 3, n_2 = 2$)	0.26	0.17	4.49	9.07

Table 2, cont. SIMPER^a results of wildlife road mortality data collected weeks 4–27 of 2020 on SH 48, SH 100, and FM 510 in Cameron County, Texas, USA. The data were sectioned into 3 observation periods: PreL (weeks 4–11), DL (weeks 12–19), and PostL (weeks 20–27). The data were transformed by $\ln(x + 1)$. Total mortality $n = 172$.

Species Group (G)	G ₁ Average Abundance	G ₂ Average Abundance	Average Dissimilarity	Contribution % ^b
Total PreL (1) and PostL (2)	4.50	2.79	49.88	99.98
Lagomorph ($n_1 = 15, n_2 = 1$)	0.90	0.09	11.69	23.43
Bird ($n_1 = 22, n_2 = 19$)	1.37	1.21	10.80	21.65
Virginia Opossum ($n_1 = 16, n_2 = 6$)	1.00	0.48	8.95	17.95
Musteloid ($n_1 = 7, n_2 = 4$)	0.57	0.31	6.51	13.04
Snake ($n_1 = 3, n_2 = 7$)	0.26	0.53	6.43	12.89
Canid ($n_1 = 5, n_2 = 2$)	0.40	0.17	5.50	11.02

^aSimilarity percentages.

^bDo not total to 100 due to rounding.

Table 3. SIMPER^a (Clarke 1993) results of road mortality surveys on Texas State Highway (SH) 48, SH 100, and Texas Farm to Market Road (FM) 510 in Cameron County, Texas, USA between 10 September 2019 and 15 June 2021. Data were transformed by $\ln(x + 1)$. Total mortality $n = 713$.

Species Group	1 Observer ($n = 46$)	2 Observers ($n = 46$)	Average Dissimilarity	Contribution % ^b
	Average Abundance	Average Abundance		
Large (Total) ($n = 362$)	1.71	2.2		41.41
Bird, Large ($n = 194$)	0.84	0.91	9.94	15.91
Virginia Opossum ($n = 107$)	0.52	0.78	7.48	11.98
Canid ($n = 34$)	0.21	0.25	4.26	6.81
Felid ($n = 16$)	0.12	0.12	2.49	3.99
Artiodactyl ($n = 11$)	0.02	0.14	1.70	2.72

^aSimilarity percentages.

^bDo not total to 100 due to rounding.

Table 3, cont. SIMPER^a results of road mortality surveys on SH 48, SH 100, and FM 510 in Cameron County, Texas, USA between 10 September 2019 and 15 June 2021. Data were transformed by $\ln(x + 1)$. Total mortality $n = 713$.

Species Group	1 Observer ($n = 46$)	2 Observers ($n = 46$)	Average Dissimilarity	Contribution % ^b
	Average Abundance	Average Abundance		
Small (Total) ($n = 247$)	1.09	1.87		40.76
Bird, Small ($n = 103$)	0.40	0.73	8.23	13.17
Lagomorph ($n = 74$)	0.29	0.57	7.23	11.57
Turtle ($n = 28$)	0.17	0.21	3.90	6.23
Rodent ($n = 22$)	0.11	0.20	3.32	5.31
Nine-banded Armadillo ($n = 20$)	0.12	0.16	2.80	4.48
Both (Total) ($n = 104$)	0.48	0.81		17.81
Musteloid ($n = 68$)	0.27	0.55	6.78	10.85
Snake ($n = 36$)	0.21	0.26	4.35	6.96

^aSimilarity percentages.

^bDo not total to 100 due to rounding.

Table 4. Statistical results of independent-samples Mann-Whitney U tests of road mortality survey counts by number of observers for all animals, large animals only, and small animals only. Surveys were performed in Cameron County, Texas, USA on Texas State Highway (SH) 48, SH 100, and Texas Farm to Market Road 510 between 10 Sep 2019 and 15 Jun 2021.

Size	n	Test Statistic (U) ^a	SE	Standardized Test Statistic (z)	P
All	92	1617	127.574	4.382	0.000
Large	92	1424	127.133	2.879	0.004
Small	92	1566	126.362	4.020	0.000

^aTests are 2-sided and asymptotic.

Table 5. Rankings of binary logistic regression models of grounded brown pelican (*Pelecanus occidentalis*) presence and absence versus weather and barrier variables versus the null (the intercept-only model) on Texas State Highway 48 in Cameron County, Texas, USA between 8 Dec 2016 and 11 March 2022.

Model ^a	AIC ^b	AIC _c ^c	w _i ^d	P
MinTmp MaxWspd AvgPres	234.7121	234.7856	0.8609	< 0.001
MinTmp MaxWspd MinPres	238.4788	238.5252	0.1309	< 0.001
AvgTmp MaxWspd AvgPres	244.5057	244.5521	0.0064	< 0.001
AvgTmp MaxWspd MinPres	247.3960	247.4424	0.0015	< 0.001
MinTmp RngWspd AvgPres	252.4425	252.4889	0.0001	< 0.001
AvgTmp RngWspd AvgPres	254.7320	254.7784	< 0.0001	< 0.001
MinTmp RngWspd MinPres	255.2156	255.2620	< 0.0001	< 0.001
MinTmp AvgWspd AvgPres	255.9679	256.0143	< 0.0001	< 0.001
MinTmp AvgWspd MinPres	256.9242	256.9707	< 0.0001	< 0.001
AvgTmp AvgWspd MinPres	270.8906	270.9370	< 0.0001	< 0.001
AvgTmp AvgWspd AvgPres	271.7709	271.8173	< 0.0001	< 0.001

^aMin = minimum, Max = maximum, Avg = average, Rng = range in. Tmp = daily air temperature (C), Wspd = daily wind speed (m/sec), Pres = daily air pressure (hectopascals).

^bAkaike information criterion.

^cCorrected Akaike information criterion.

^dAkaike weight value.

Table 6. Parameters of the top-ranked binary logistic regression model of grounded brown pelican (*Pelecanus occidentalis*) presence and absence versus weather and barrier variables versus the null (the intercept-only model) on Texas State Highway 48 in Cameron County, Texas, USA between 8 Dec 2016 and 11 March 2022. This model was significant ($\chi^2 = 89.215, P \leq 0.001$). $n = 867$.

Parameter ^b	Parameter Estimates						
	B ^c	SE	95% Wald CI for B ^a		Hypothesis Test		
			Lower	Upper	Wald χ^2	df	P
(Intercept)	108.975	36.3299	37.770	180.180	8.998	1	0.003
Daily minimum air temperature (C)	-0.202	0.0368	-0.274	-0.130	30.264	1	< 0.001
Daily maximum wind speed (m/sec)	0.505	0.0765	0.355	0.655	43.581	1	< 0.001
Daily average air pressure (hectopascals)	-0.112	0.0353	-0.181	-0.043	10.039	1	0.008

^aBeta coefficient.

^bThe scale and ancillary parameters were set to 1.

^cOdds ratios are calculated by the formula e^B .

Table 7. Rankings of negative binomial regression models of grounded brown pelican (*Pelecanus occidentalis*) counts versus weather and barrier variables versus the null (the intercept-only model) on Texas State Highway 48 in Cameron County, Texas, USA between 8 Dec 2016 and 11 March 2022. $n = 42$.

Model ^a	AIC ^b	AIC _c ^c	w_i ^d	<i>P</i>
T2P MinTmp AvgPres	329.5534	330.6345	0.3656	< 0.001
MinTmp AvgPres T2P AvgWspd	329.5755	331.2421	0.2670	< 0.001
MinTmp MaxWspd AvgPres T2P	330.3178	331.9845	0.1861	< 0.001
AvgPres T2P AvgTmp	332.7116	333.7927	0.0754	< 0.001
MinTmp T2P	334.5299	335.1615	0.0380	< 0.001
MinTmp T2P AvgWspd	335.4675	336.5486	0.0194	0.001
T2P	336.3247	336.6324	0.0182	< 0.001
T2P MinPres MinTmp	336.2435	337.3246	0.0129	0.001
T2P MinTmp AvgTmp	336.4922	337.5732	0.0114	0.001
T2P MinPres MinTmp MaxWspd	338.1748	339.8415	0.0037	0.003

^aMin = minimum, Max = maximum, Avg = average. Tmp = daily air temperature (C), Wspd = daily wind speed (m/sec), Pres = daily air pressure (hectopascals), T2P = T2P railing.

^bAkaike information criterion.

^cCorrected Akaike information criterion.

^dAkaike weight value.

Table 8. Parameters of the top-ranked negative binomial regression model of grounded brown pelican (*Pelecanus occidentalis*) counts versus weather and barrier variables versus the null (the intercept-only model) on Texas State Highway 48 in Cameron County, Texas, USA between 8 Dec 2016 and 11 March 2022. $n = 42$.

Parameter ^b	Parameter Estimates						
	B	SE	95% Wald CI for B ^a		Hypothesis Test		
			Lower	Upper	Wald χ^2	df	<i>P</i>
(Intercept)	134.961	48.3716	40.155	229.768	7.785	1	0.005
Daily minimum air temperature (C)	-0.099	0.0313	-0.161	-0.038	10.041	1	0.002
Daily average air pressure (hectopascals)	-0.128	0.0472	-0.220	-0.035	7.337	1	0.007
T2P Railing	-1.644	0.3601	-2.350	-0.938	20.847	1	0.000

^aBeta coefficient.

^bThe beta coefficient of concrete traffic barrier was set to 0 because the parameter is redundant (and so is not displayed) and the scale and ancillary dispersion parameters were set to 1.

Table 9. GoPro Hero9 Black (GoPro, Inc., San Mateo, CA, USA) settings and survey vehicle speeds compared to determine optimal road mortality video survey methodology.

Settings Number	Camera Settings				
	Horizontal/Vertical FOV ^a	HyperSmooth	Digital Lens	FPS ^b	Resolution ^c
1	87°/56°	High	Linear	60	4k
2	87°/56°	High	Linear	120	2.7k
3	87°/56°	On	Linear	60	4k
4	87°/56°	On	Linear	120	2.7k
5	92°/61°	Off	Linear	60	4k
6	92°/61°	Off	Linear	120	2.7k
7	109°/63°	High	Wide	60	4k
8	109°/63°	High	Wide	120	2.7k

^aField of view.

^bFrames per second.

^c4k resolution is 3,840 by 2,160 pixels and 2.7k resolution is 2,704 by 1,524 pixels.

Table 9, cont. GoPro Hero9 Black settings and survey vehicle speeds compared to determine optimal road mortality video survey methodology.

Settings Number	Camera Settings				
	Horizontal/Vertical FOV ^a	HyperSmooth	Digital Lens	FPS ^b	Resolution ^c
9	109°/63°	On	Wide	60	4k
10	109°/63°	On	Wide	120	2.7k
11	118°/69°	Off	Wide	60	4k
12	118°/69°	Off	Wide	120	2.7k
13	113°/86°	On	Superview	30	4k
14	113°/86°	On	Superview	60	2.7k
15	121°/93°	Off	Superview	30	4k
16	121°/93°	Off	Superview	60	2.7k

^aField of view

^bFrames per second

^c4k resolution is 3,840 by 2,160 pixels and 2.7k resolution is 2,704 by 1,524 pixels.

APPENDIX B

APPENDIX B

FIGURES

Figure 1. Map of the roads surveyed by the lab of Dr. Richard Kline for wildlife road mortalities in south Texas, USA: Texas State Highway (SH) 48, SH 100, Texas Farm to Market Road (FM) 510, and FM 106 (Esri Inc., Redlands, CA, USA; HERE North America LLC, Chicago, IL, USA; Garmin Ltd., Schaffhausen, Switzerland). Wildlife crossing structures are located on SH 48, SH 100, and FM 106. FM 106 happened to be excluded from all analyses as surveys there began only Aug 2020. Only portions of the road that were surveyed are outlined (red). A map highlighting Cameron County within Texas is inset (National Atlas of the United States, US Department of the Interior, Washington, D.C., USA).

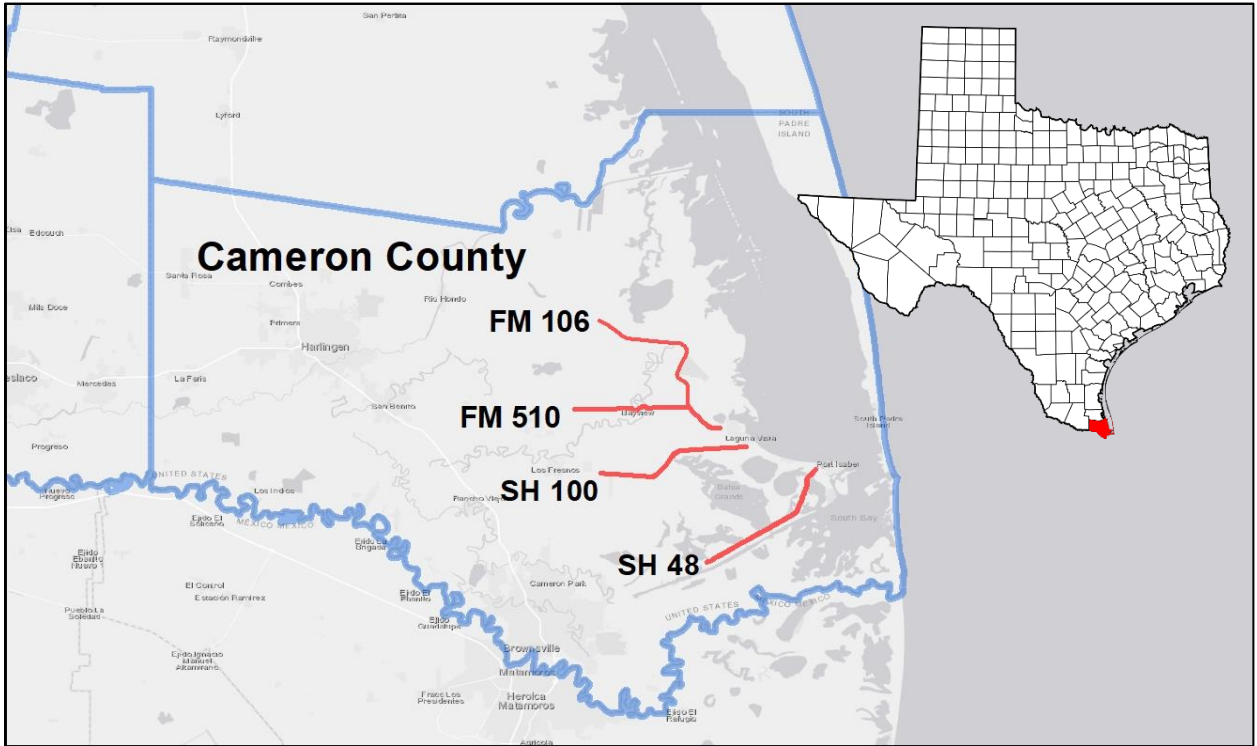


Figure 2. Results of independent-samples median tests of road mortality survey counts by number of observers for (a) large animals only, (b) small animals only, and (c) all animals. Surveys were performed in Cameron County, Texas, USA on Texas State Highway (SH) 48, SH 100, and Texas Farm to Market Road 510 between 10 Sep 2019 and 15 Jun 2021. Circles indicate outliers and asterisks indicate extreme outliers ($> \text{Quartile } 3 + 3 \times \text{Interquartile Range}$). Total $n = 92$. Medians of counts by number of observers differ for each: (a) $\chi^2_{(0.05, 1)} = 7.379, P \leq 0.001$, (b) $\chi^2_{(0.05, 1)} = 12.619, P < 0.01$, (c) $\chi^2_{(0.05, 1)} = 15.883, P \leq 0.001$.

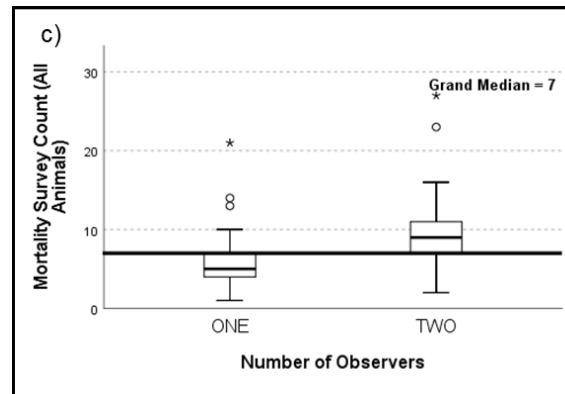
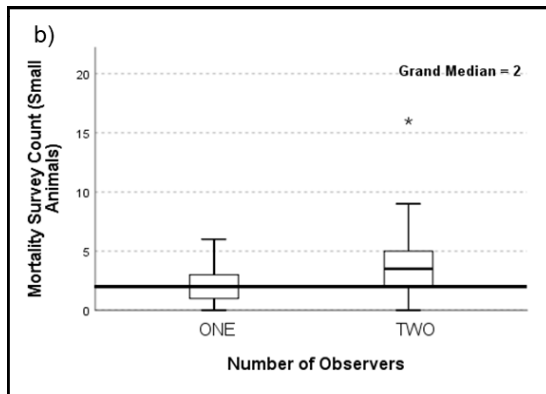
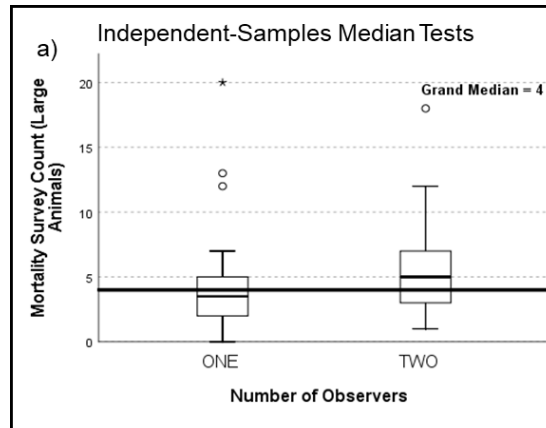


Figure 3. Number of road mortality surveys in Cameron County, Texas, USA, on Texas State Highway (SH) 48, SH 100, Texas Farm to Market Road (FM) 510, and FM 106 per month by number of observers between 10 September 2019 and 15 June 2021.

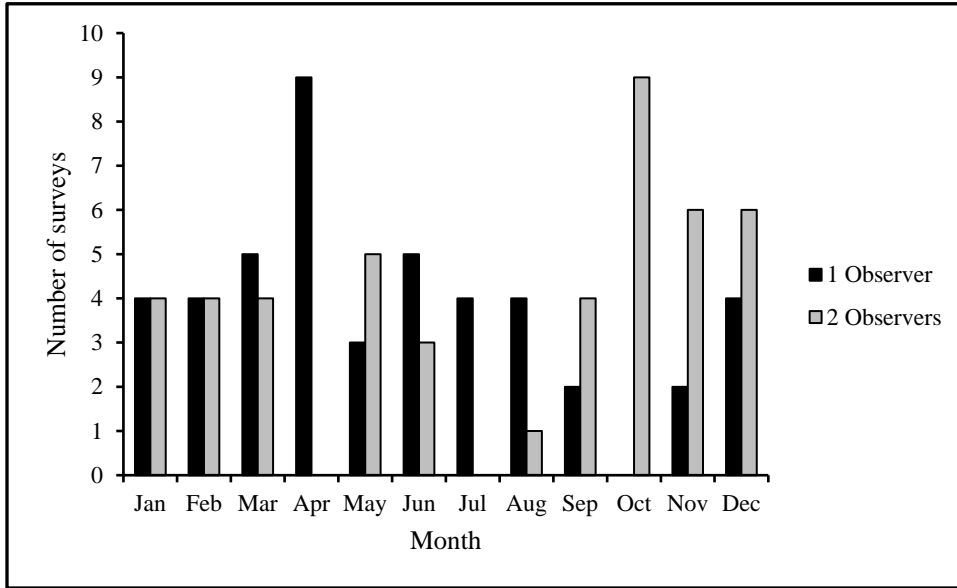


Figure 4. Map of brown pelican (*Pelecanus occidentalis*) mortality density (pelicans/hectare (ha)) on Texas State Highway 48 in Cameron County, Texas, USA recorded during road mortality surveys Apr 2019 through Feb 2022. Values are rounded to 2 significant digits after the decimal. Seventy pelican mortalities were recorded during this period. All but 1 were in the vicinity of the Carl “Joe” Gayman Bridge (1 was near the San Martin Bridge). Basemap provided by Earthstar Geographics LLC (San Diego, CA, USA) and Maxar Technologies Inc. (Westminster, CO, USA).

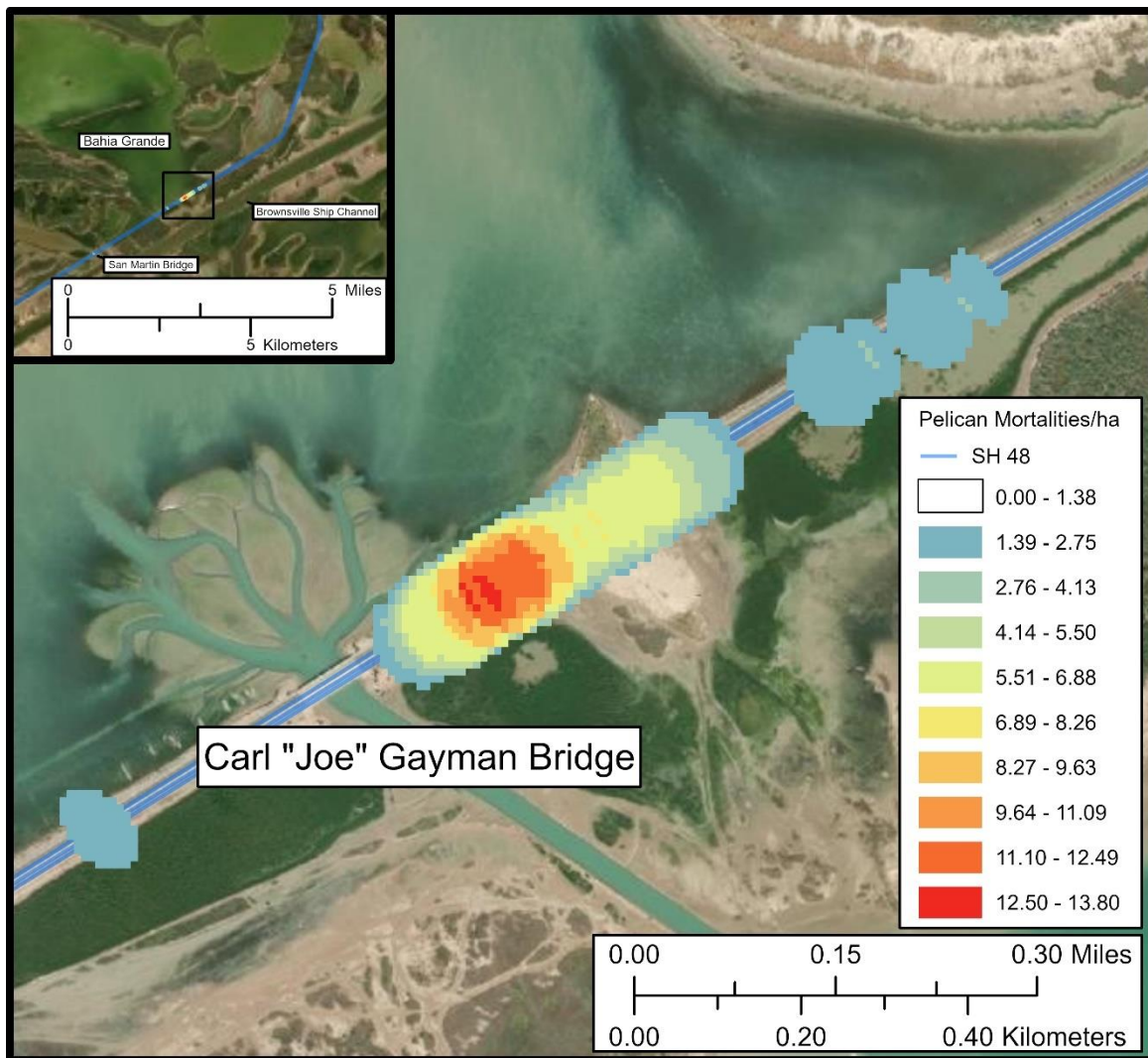


Figure 5. Example section of concrete traffic barrier (median barrier pictured) and T2P railing (side barriers pictured) with metal poles extensions (which were kept through the transition from concrete to T2P). The road pictured is Texas State Highway 48 in Cameron County, Texas, USA.



Figure 6. A drawing of a section of T2P railing. They have a 9-inch concrete parapet with a round steel-top tube and 2 rectangular steel tubes. The rails are supported by twin steel posts spaced a maximum of 8 feet apart. They have a nominal height of 33 inches and a minimum height of 31 inches after maintenance overlays (Texas Department of Transportation 2020).

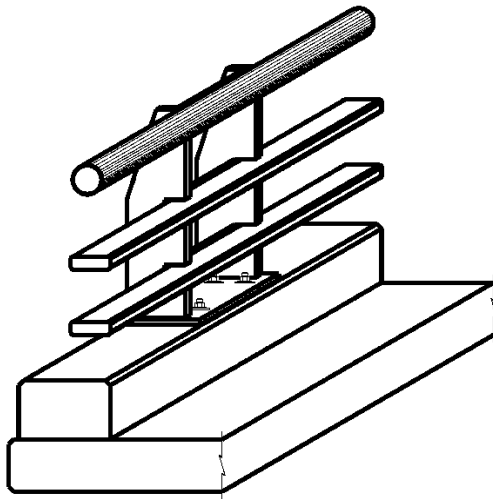


Figure 7. Comparison of brown pelican (*Pelecanus occidentalis*) mortalities recorded on road mortality surveys (blue) and pelican groundings recorded by citizen scientists (orange). Data ranges 8 Dec 2016 through 28 Feb 2022 and excludes all dates 7 Apr through 31 Aug as no mortalities or groundings were recorded in that range during any year. The x-axis is labeled every 28 days. Road mortality surveys only began including brown pelicans 19 Dec 2016. The citizen science data encompassed all major spikes in pelican mortalities. Sampling for the citizen science dataset occurred when pelican mortalities were expected to potentially occur, in contrast to the weekly road mortality surveys.

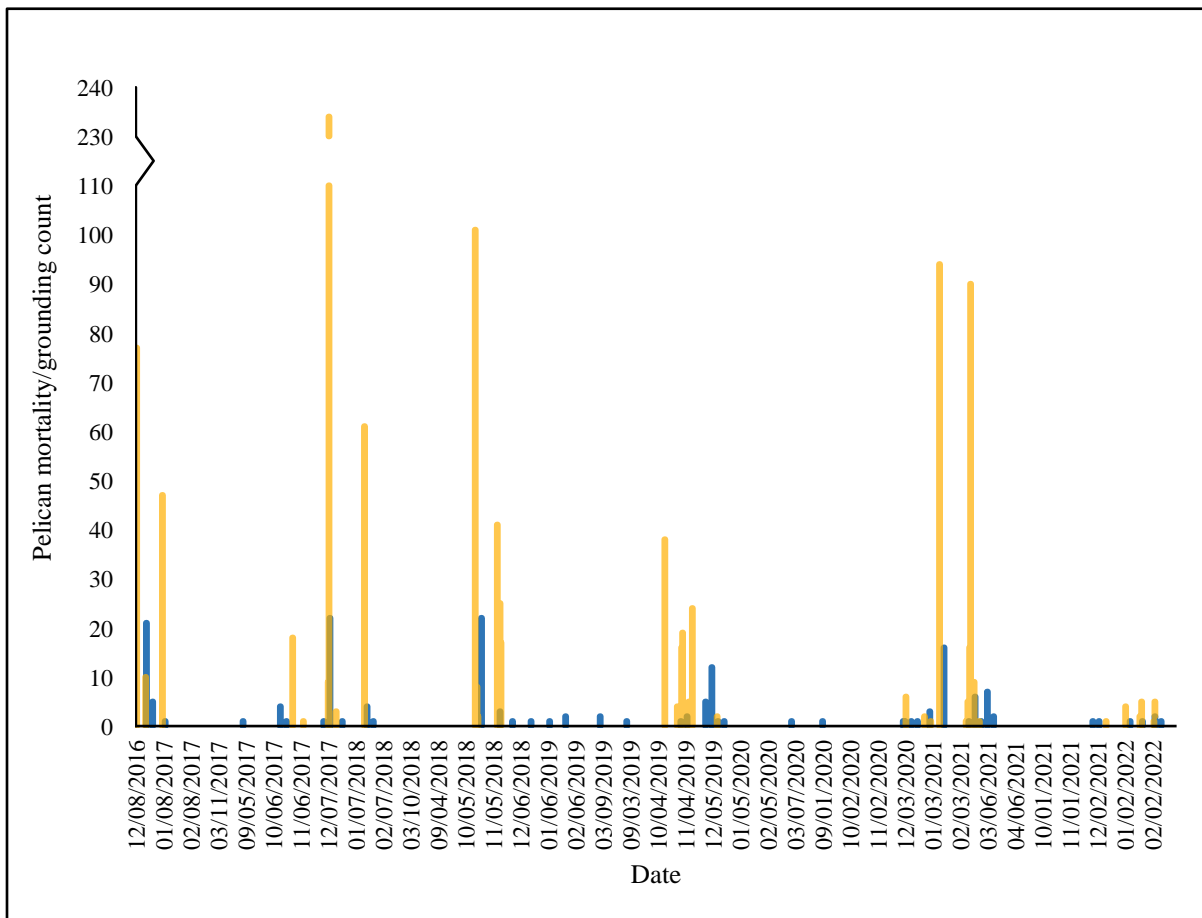


Figure 8. Representative plots of wind (a) and air temperature (b) variable values recorded by National Oceanic and Atmospheric Administration station PTIT2 (2022). They were compared for use in analysis of brown pelican (*Pelecanus occidentalis*) groundings on Texas State Highway 48 in Cameron County, Texas, USA. The selected range is 8 Jan 2019 through 25 Nov 2019. Numbers of grounded brown pelicans recorded by citizen scientists are also displayed.

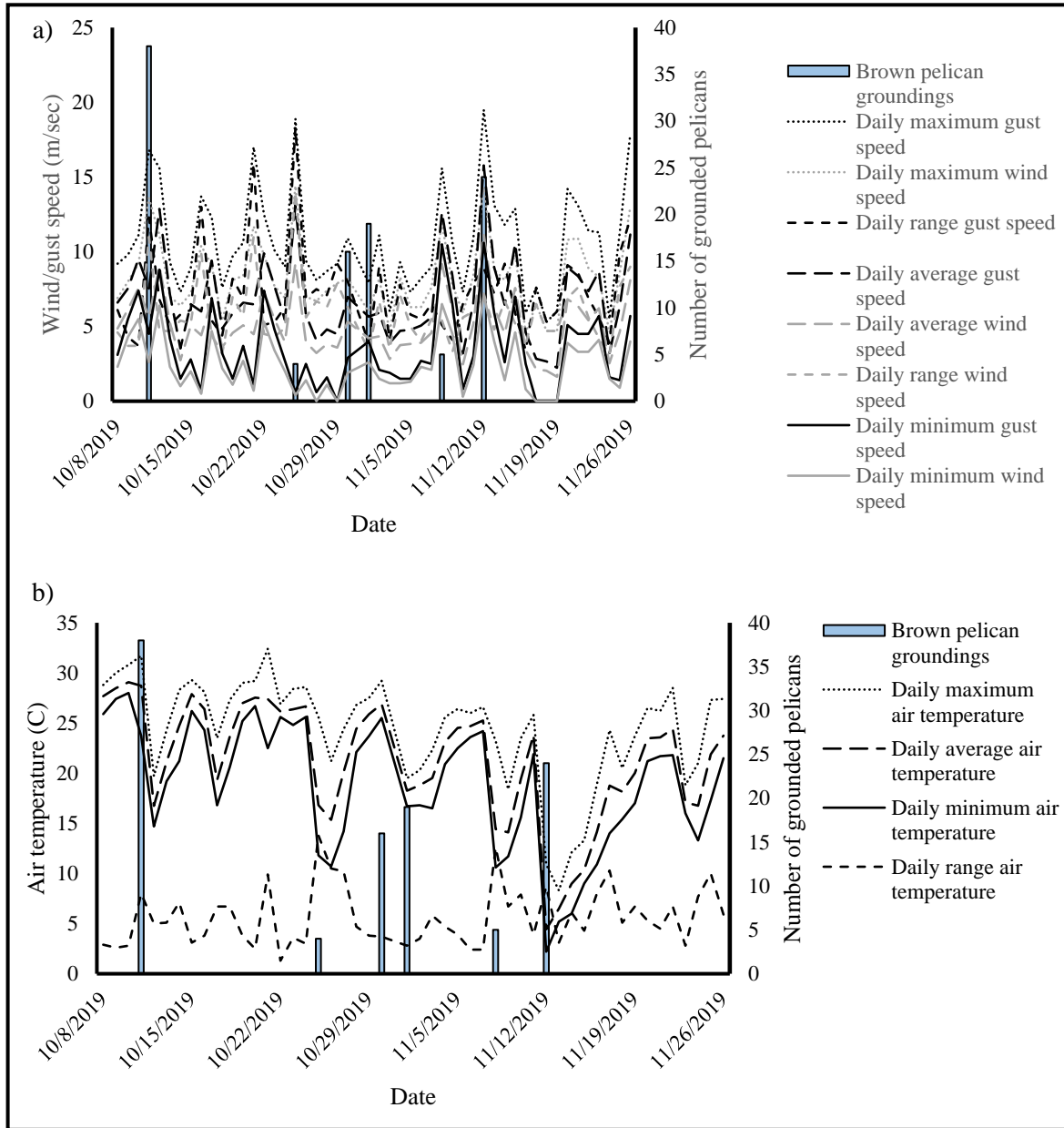


Figure 9. Scatterplots of predicted means generated through negative binomial regression of number of grounded brown pelicans (*Pelecanus occidentalis*) on Texas State Highway 48 in Cameron County, Texas, USA, between 8 Dec 2016 and 11 Mar 2022 versus (a) type of traffic barrier on the sides of the road, (b) daily average air pressure, and (c) daily minimum air temperature. All the predicted mean data trend negatively.

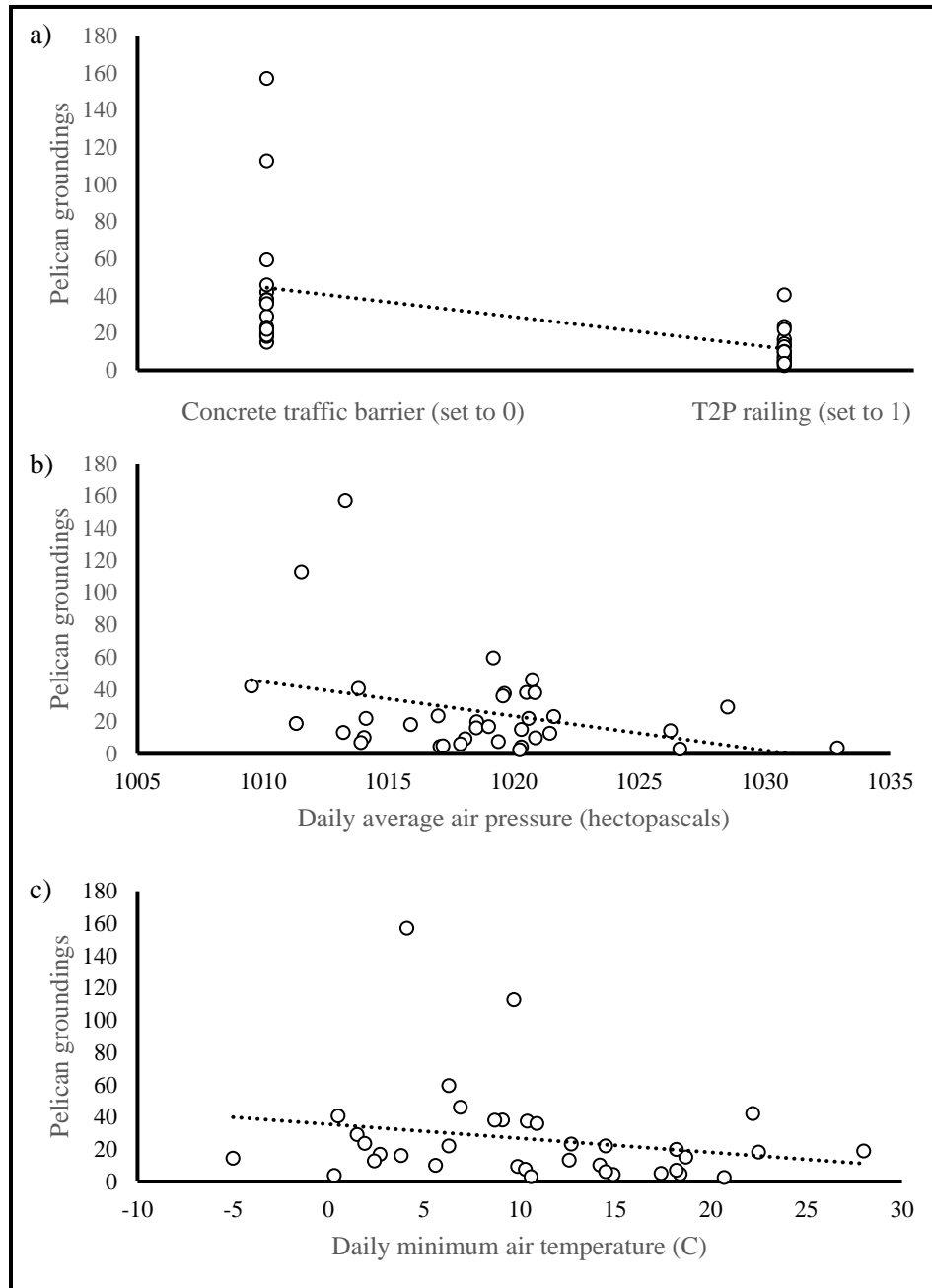


Figure 10. Camera positions and mounts used by Livingston (2019) for road mortality video surveys. Both cameras were mounted with suction cup mounts. Position 1 is on the outside of the driver's side of the windshield pointing down and forward toward the left of the vehicle. Position 2 is on the front right side of the hood and is angled forward and slightly down and to the right.



Figure 11. Camera positions tested for improving road mortality video surveys. Positions 1a, 2a, 3a, and 4a used suction cup mounts. Positions 5a, 6a, 1b, and 2b used GoPro Jaws: Flex Clamp mounts (GoPro, Inc., San Mateo, CA, USA). Positions 7a, 8a, and 3b used flat adhesive mounts (7a and 3b atop poles). Position 4b used a magnetic mount. Position 1a, 3a, 3b, and 4b cameras faced forward, angled slightly down and left. The position 2a camera faced forward, angled slightly down and right. Position 4a, 5a, 6a, and 7a cameras faced right, angled down. The position 8a camera faced forward. Position 1b and 2b cameras faced left, angled slightly down.

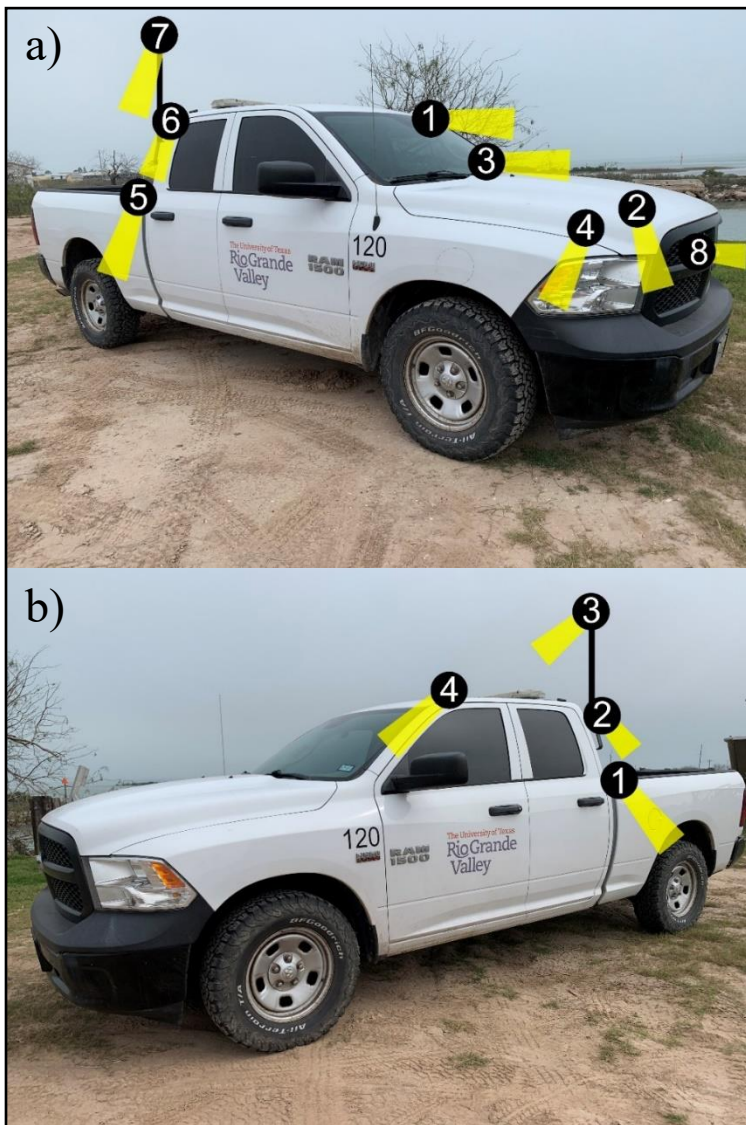


Figure 12. Field of view (FOV) comparison of camera positions 3b (a) and 4b (b). Weighted cardboard boxes with Snellen eye charts are the targets of these screenshots. More of the side profile is visible with position 4b. Positions 3b and 4b provided the best 2 front-facing FOV.

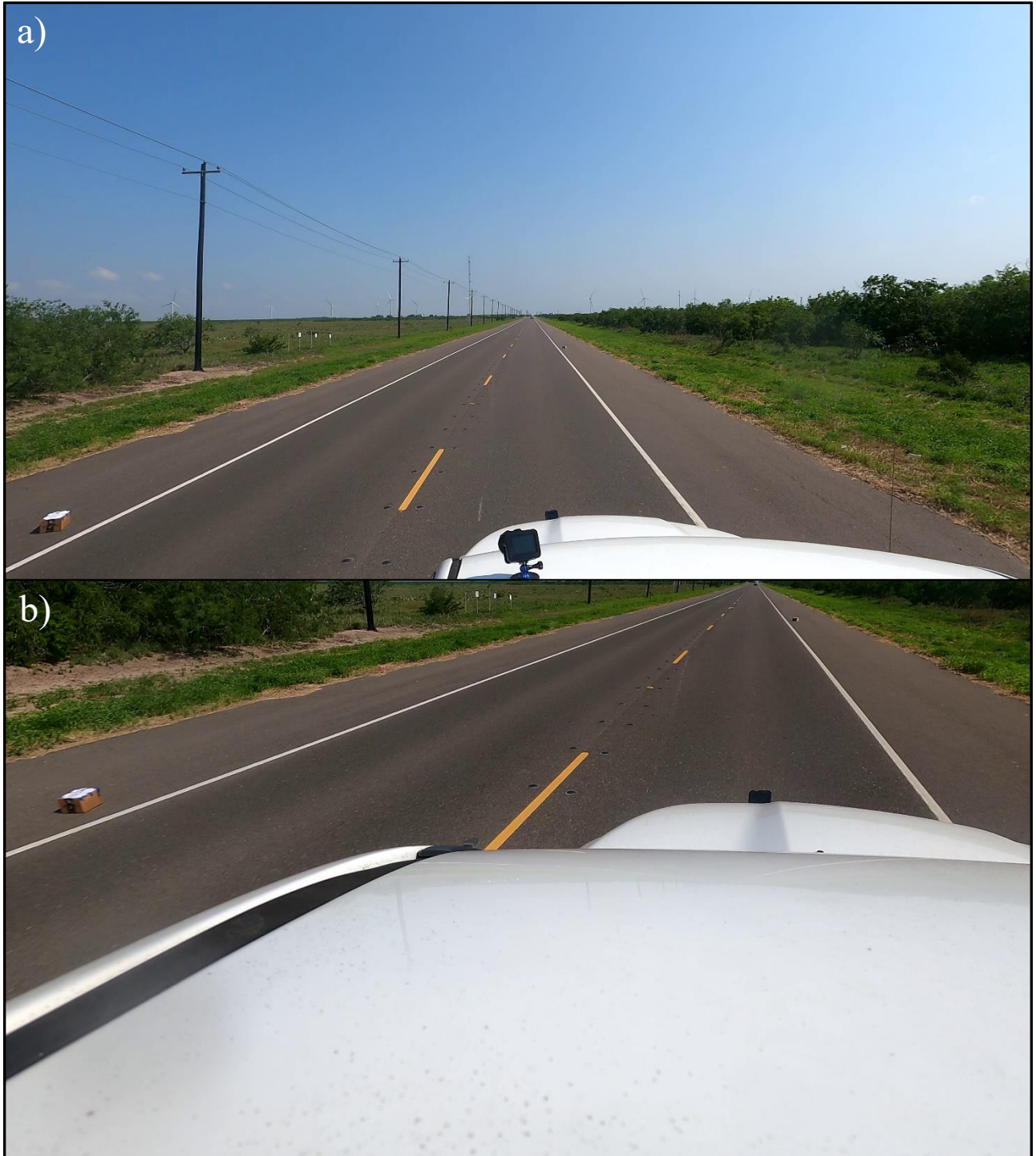


Figure 13. Field of view (FOV) comparison of camera positions 6a (a) and 7a (b). Weighted cardboard boxes with Snellen eye charts are the targets of these screenshots. Position 7a provides more top-down coverage. Positions 6a and 7a provided the best 2 right-facing FOV.



Figure 14. Camera position 1a field of view (FOV) (a) versus position 4b FOV (b), both showing a raccoon (*Procyon lotor*) in the left shoulder. Relative quality of position 1a is skewed between these two images as the speed of the vehicle was lower for the position 1a image. Position 4b provides more top-down coverage.

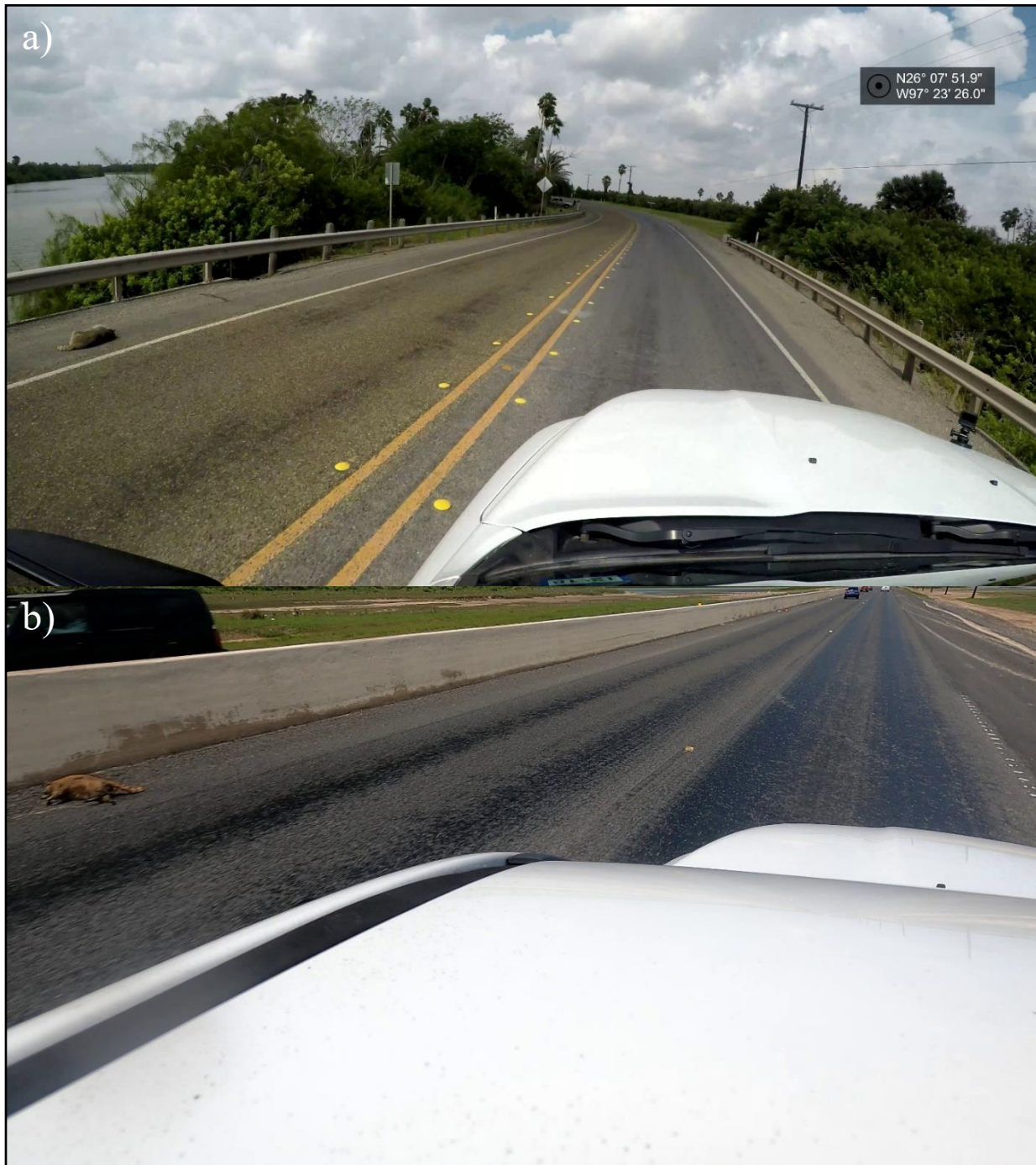


Figure 15. Camera position 2a (a) field of view (FOV) versus camera position 7a FOV (b), both showing a raccoon (*Procyon lotor*) in the left shoulder. Camera position 7a provides a far better angle at which to view the mortality.



Figure 16. Example fields of view of best front-facing (c, d) and right-facing (a, b) camera positions at 64 km/hr (a, c) versus at 89 km/hr (b, d). The front-facing camera pictures are of a Snellen eye chart taped to the road (Texas Farm to Market Road (FM) 510) by the midline. The right-facing camera pictures are of a Snellen eye chart taped to a weighted cardboard box in the middle of the right shoulder of the road (FM 510).

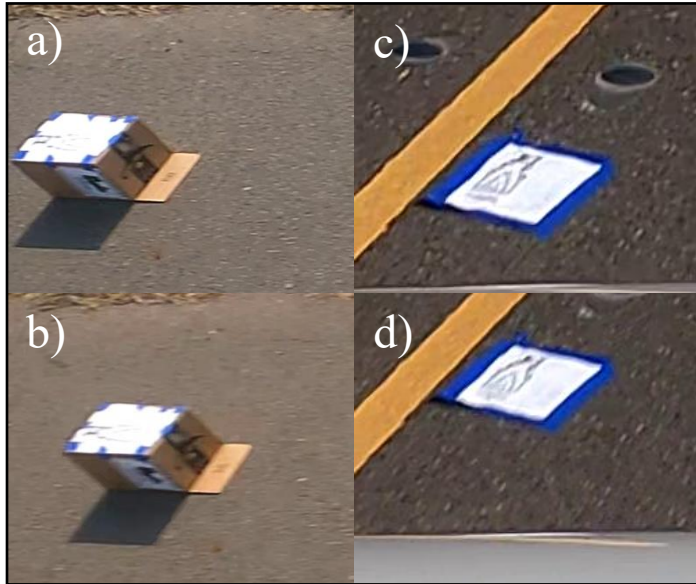


Figure 17. Screenshot displaying DroneViewer's interactable GPS track.



BIOGRAPHICAL SKETCH

Bradley Beer was raised in Coral Springs, Florida. He graduated the University of Florida in May 2018 with a Bachelor of Science in Wildlife Ecology and Conservation. In December 2022 he graduated the University of Texas Rio Grande Valley with a Master of Science in Biology under Dr. Richard J. Kline. He may be contacted via his personal email address: bradleybeer@gmail.com.